LUND UNIVERSITY

Synthesis of a Model-based Tire Slip Controller

Solyom, Stefan

2002

Document Version:
Publisher's PDF, also known as Version of record

Link to publication

Citation for published version (APA):
Solyom, S. (2002). *Synthesis of a Model-based Tire Slip Controller*. [Licentiate Thesis, Department of Automatic Control]. Department of Automatic Control, Lund Institute of Technology (LTH).

Total number of authors:
1

General rights
Unless other specific re-use rights are stated the following general rights apply:
Copyright and moral rights for the publications made accessible in the public portal are retained by the authors and/or other copyright owners and it is a condition of accessing publications that users recognise and abide by the legal requirements associated with these rights.
• Users may download and print one copy of any publication from the public portal for the purpose of private study or research.
• You may not further distribute the material or use it for any profit-making activity or commercial gain
• You may freely distribute the URL identifying the publication in the public portal

Read more about Creative commons licenses: https://creativecommons.org/licenses/

Take down policy
If you believe that this document breaches copyright please contact us providing details, and we will remove access to the work immediately and investigate your claim.

LUND UNIVERSITY

PO Box 117
221 00 Lund
+46 46-222 00 00

Synthesis of a Model-based Tire Slip Controller

Stefan Solyom

Department of Automatic Control
Lund Institute of Technology
Lund, Sweden

Department of Automatic Control
Lund Institute of Technology
Box 118
SE-221 00 Lund Sweden

Document name
LICENTIATE THESIS

Date of issue
June 2002

Document Number
ISRN LUTFD2/TFRT--3228--SE

Author(s)
Stefan Solyom

Supervisor
Anders Rantzer
Björn Wittenmark

Sponsoring organisation
ESPRIT–H2C

Title and subtitle
Synthesis of a Model-based Tire Slip Controller

Abstract

The Anti-lock Braking System (ABS) is an important component of a complex steering system for the modern car. In the latest generation of brake-by-wire systems, the performance requirements on the ABS have changed. The controllers have to be able to maintain a specified tire slip for each wheel during braking. This thesis proposes a design model and based on that a hybrid controller that regulates the tire-slip. Simulation and test results are presented.

A design method for robust PID controllers is presented. Robustness is ensured with respect to a cone bounded static nonlinearity acting on the plant. Additional constraints on maximum sensitivity are also considered. The design procedure has been successfully applied in the synthesis of the proposed hybrid ABS controller.

Trajectory convergence for a class of nonlinear systems is analyzed. The servo problem for piecewise linear systems is treated. Convex optimization is used to describe the behavior of system trajectories of a piecewise linear system with respect to some input signals.

Key words
ABS, synthesis, hybrid, PID, piecewise linear, LMI

Classification system and/or index terms (if any)

Supplementary bibliographical information

ISSN and key title
0280–5316

ISBN

Language
English

Number of pages
74

Recipient's notes

Security classification

The report may be ordered from the Department of Automatic Control or borrowed through:
University Library 2, Box 3, SE-221 00 Lund, Sweden
Fax +46 46 222 44 22 E-mail ub2@ub2.lu.se

Synthesis of a Model-based Tire Slip Controller

Stefan Solyom

Department of Automatic Control
Lund Institute of Technology
Lund, June 2002

Department of Automatic Control
Lund Institute of Technology
Box 118
S-221 00 LUND
Sweden

ISSN
ISRN LUTFD2/TFRT--3228--SE

©2002 by Stefan Solyom. All rights reserved.
Printed in Sweden,
Lund University, Lund 2002

Contents

Acknowledgments

First of all I would like to thank my supervisor Professor Anders Rantzer for his guidance and support. He was a great source of inspiration from the moment I met him, more than three years ago. His influence during these years has profoundly contributed to the value of this thesis.

Many thanks to Andrey Ghulchak for his excellent courses and inspiring discussions, as well as his patience in answering so many questions of mathematical nature.

I am grateful to Professor Björn Wittenmark and Professor Tore Hägglund for their valuable comments and suggestions regarding the manuscript.

I would like to express my appreciation to the team at Daimler-Chrysler that made possible the real-life testing of this work. In particular, to Dr. Jens Kalkkuhl at DaimlerChrysler for inspiring discussions and insightful suggestions regarding the work in the second chapter of this thesis.

Sincere gratitudes to Professor Stefan Preitl and Professor Paul M. Frank who made possible my first more profound contact with the field of control during my master thesis.

It has also been grate fun to work together with Ari Ingimundarson on the problems presented in Chapter 3 of this thesis.

I would like to thank all my colleagues at the department for their support. It is elevating to be part of such a great collective. Special thanks to Leif Andersson for his help in any computer related questions that appeared in these years.

Financial support from the EU-Esprit project Heterogeneous Hybrid Control ($\mathcal{H}^2\mathcal{C}$) is gratefully acknowledged.

Finally I would like to thank my parents for their understanding and support and to Diana for her patience and encouragement.

Stefan

1

Introduction

1.1 Background and Motivation

One of the most important subsystems in any vehicle is its braking system. In the last century, braking systems evolved considerably. It started with primitive systems, consisting of a block rubbing against the wheel rim. Today, the braking is electronically controlled by Anti-lock Braking Systems (ABS).

"While the development of braking systems has come a long way, the progress is just beginning." [Buckman, 1998]

The first ABS systems were implemented in the late 1970's, the main objective of the control system being prevention of wheel-lock. Most ABS controllers available on the market are table and relay-feedback based, making use of hydraulic actuators to deliver the braking force.

In the latest generation of brake-by-wire systems, electro-mechanic actuators are capable of delivering continuously varying and different brake forces independently to the four wheels. Such actuators are capable of superior performance, needing novel slip controllers that can fully exploit these capabilities. The control objective of these systems shifts to maintain a specified tire slip rather then just preventing wheel-lock. The set-point slip is supposed to be provided by a higher level in the hierarchy (e.g. an ESP system), and can be used for sta-

bilizing the steering dynamics of the car while braking.

This thesis proposes a novel gain-scheduling scheme for tire slip control. This controller has the capability of controlling the tire slip at a given set-point.

To tune the proposed controller, new theory has been developed. The proposed synthesis method can be used for a wide class of nonlinear systems.

During the synthesis of the controller, an important factor was the servo properties of the control system. Motivated by this, the servo problem for a special type of nonlinear systems is examined.

1.2 Contributions and Related Publications

Chapter 2 of this thesis is concerned with an industrial application, an Anti-lock Braking System for a passenger vehicle. A novel control system is proposed. Simulation and test results are presented. The work in this chapter is contained in:

Solyom, S. and A. Rantzer (2002): "ABS Control by Gain Scheduling." *To be published in Nonlinear and Hybrid Control in Automotive Applications, Springer-Verlag*.

The third chapter is treating a synthesis method for robust PI(D) controllers. This design method is used to tune the nonlinear controller developed in the second chapter. The work in this chapter is contained in:

Solyom, S. and A. Ingimundarson (2002): "A synthesis method of robust PID controllers for a class of uncertainties." *Accepted for publication in Asian Journal of Control, Special Issue on PID Control*.

The fourth chapter is treating the servo problem for piecewise linear systems. Convex optimization is used to describe the behavior of system trajectories of a piecewise linear system with respect to some input signals. The work in this chapter is contained in:

Solyom, S. and A. Rantzer (2002b): "The servo problem for piecewise linear systems." *Accepted at 15th International Symposium on Mathematical Theory of Networks and Systems, Notre Dame*.

1.3 Future Work

In the first part of this thesis a model based Anti-lock Braking System is presented. Simulation and test results are presented. In order to fully validate the proposed controller, more tests are needed, especially for low friction surfaces. Furthermore, in the control design only longitudinal slip has been considered. It is the believe of the author that the controller can be easily adapted for the cases when side-slip is present.

The third chapter of the thesis treats a synthesis procedure for PID controllers for a class of uncertain systems. It solves the problem for a cone bounded nonlinearity in feedback with a part of the plant. It is of interest to investigate the case when multiple cone bounded nonlinerities are present in the system.

The last chapter presents a result for analysis of piecewise linear systems. Behavior of system trjectory is analyzed with respect to some input signal. In the current stage of the result, the input signal at each time instant is constrained to a set. It is of interest to relax this constraint such that the equilibrium point of the piecewise linear system can switch partition.

2

ABS control — A design model and control structure

2.1 Introduction

The Anti-lock Braking System (ABS) is an important component of a complex steering system for the modern car. It is now available on most of the vehicles, enhancing their braking capabilities.

The early development of anti-lock system for vehicle brakes began in Europe in the mid 1920's [Buckman, 1998]. One of the first patents in Europe was issued in 1932 entitled "An Improved Safety Device for Preventing the Jamming of the Running Wheels of Automobiles when Braking". In the US the first patent was issued in 1936, named "Apparatus for Preventing Wheel Sliding". Contrary to the common belief, the first practical application of an anti-lock system to a vehicle was done to railroad trains and not to aircrafts. The first occurred around 1943, while the later appeared in the late 1940's and early 1950's. In 1951 an anti-lock braking system for highway vehicles was presented. These early systems were mechanical systems and performed with varying degrees of efficiency, but they significantly improved vehicle steerability during braking. This ability of the early sys-

tems encouraged further development. In 1968 an optional equipment for Thunderbirds was a rear axle hydraulic ABS. The control algorithm of this system was implemented on analog computers with primarily discrete components, resulting in low reliability. In 1978, Mercedes-Benz offered anti-lock braking system as an optional equipment for its S-class vehicles. In the beginning of the 1980's the algorithms were migrated to micro-computers and ABS development started to progress strongly. By 1985, Mercedes, BMW and Audi introduced Bosch ABS systems. Meanwhile Ford introduced its first Teves systems. In the late 1980's ABS systems were offered on many luxury and sports cars. Today, ABS systems can be found on most of the vehicles, tending to be a standard equipment.

The main objective of most of these control system is prevention of wheel-lock while braking. This is important for two main reasons. First, to maintain steering ability of the car while hard and emergency braking, enabling obstacle avoidance in such situations. Second, to decrease the braking distance in case of an emergency braking. The later is due to the fact that the maximum friction between the road and the tires is, in most of the cases, achieved when the wheel is still rotating and not when is locked.

It turns out that this task is not trivial, one of the main reasons being the high amount of uncertainty involved. Most uncertainty arises from the friction between the tires and the road surface. In addition, the tire-road characteristics is highly nonlinear, which burdens even further the control task.

The brake actuators play an important role in slip control, influencing the control system's performance. Most of the ABS available on the market are making use of hydraulic actuators. These are simple hydraulic valves, usually with three-point-characteristics. In the new generation of ABS, electro-hydraulic actuators are used and in the next generation of brake-by-wire systems electro-mechanic actuators will be used. In a brake-by-wire system the drivers action on the brake pedal is converted into electrical signals that are transmitted via microcontrollers to the brake actuators. This way there is no hydraulic connection between the pedal and the actuators. The brake actuators used in these systems have the advantage of allowing continuous and more accurate adjustment of the brake force. These braking systems enable control of tire slip at arbitrary set-points which can be

used to improve the driving characteristics of the vehicle. This means that to fully exploit the capabilities of such braking systems, there is a need for new high performance control systems. In particular, these controllers should be able to regulate the slip at different set-points. These reference values are to be specified by other systems, such as an Electronic Stabilization Program (ESP).

The key word for novel vehicle dynamics control systems is integration. Different levels, in a hierarchical structure of controllers with different functionalities are interacting in order to improve the driving characteristics of the vehicle. Such a high level integration and interaction is not possible without brake-by-wire technology. To fully use the capabilities offered by this technology, new analysis and synthesis approaches are to be developed.

This chapter is addressing the ABS system for a vehicle equipped with brake-by-wire technology. A novel, model based control approach for slip control is proposed. A systematic synthesis method is proposed. The resulting controller is a hybrid nonlinear PID controller. Tests have been carried out in a Mercedes E220 vehicle, provided by Daimler-Chrysler, equipped with electro-mechanical brakes and brake-by-wire system.

2.2 Process description

It is easiest to understand the underlying control problem by looking at the so called quarter car model. This model consists of a single wheel attached to a mass, as shown in Figure 2.1.

The equations of motion of the quarter car, in case of braking, are given by:

$$\begin{aligned} J\dot{\omega} &= rF_x - T_b \\ m\dot{v} &= -F_x \end{aligned} \tag{2.1}$$

where:

m - mass of the quarter car

v - velocity over ground of the car

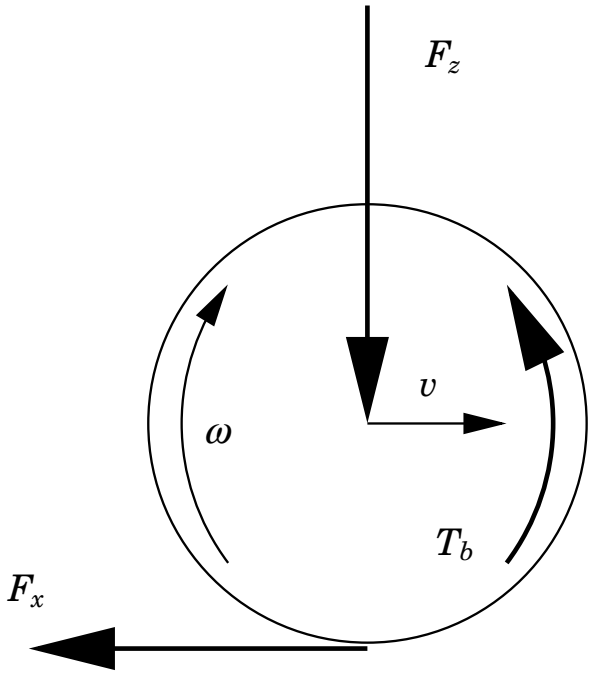

Figure 2.1 Quarter car.

ω - angular velocity of the wheel

F_z - vertical force

F_x - tire friction force

T_b - brake torque

r - wheel radius

J - wheel inertia

The longitudinal tire slip is defined as:

$$\lambda = \frac{v - \omega r}{v} \tag{2.2}$$

hence, a locked wheel ($\omega = 0$) is described by $\lambda = 1$, while the free motion of the wheel ($\omega r = v$) is described by $\lambda = 0$.
The tire friction force, F_x, is determined by:

$$F_x = F_z \mu(\lambda, \mu_H, \alpha, F_z, v)$$

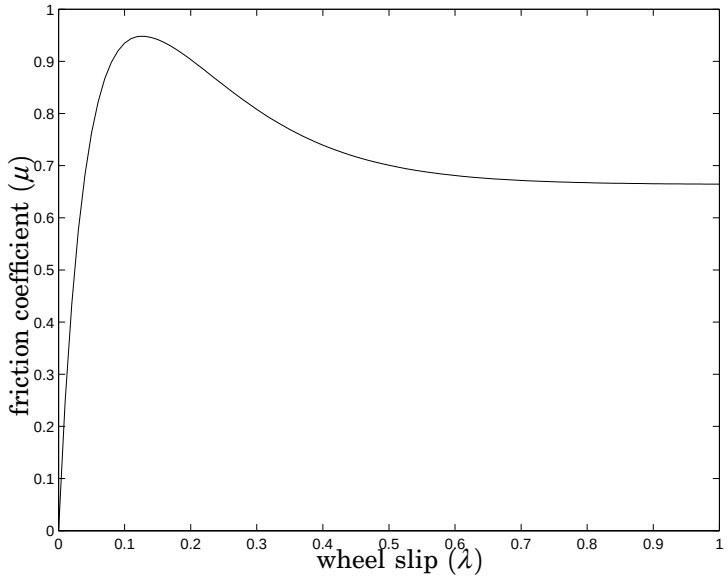

Figure 2.2 Tire friction curve.

where $\mu(\lambda, \mu_H, \alpha, F_z)$ is the road-tire friction coefficient, a nonlinear function with a typical dependence on the slip shown in Figure 2.2 (μ_H denotes the maximum friction coefficient). The most common tire friction model used in the literature is the "Magic Formula" [Bakker *et al.*, 1989], or Pacejka model. This model uses static maps to describe the dependence between slip and friction and it can depend on the vehicles velocity (v). In the literature there are reported several dynamical friction models [Bliman *et al.*, 1995], [Canudas de Wit and Tsiotras, 1999], that attempt to capture more accurately the transient behavior of the tire-road contact forces. In this work a Pacejka model will be used for simulations as well as design. This function depends also on the normal force (F_z), steering angle (α), road surface, tire characteristics, velocity of the car. For ease of writing, in the following the arguments of μ will be dropped. Substituting (2.2) into (2.1), the system becomes:

$$\begin{aligned} \dot{\lambda} v &= -\frac{F_z \mu}{J} r^2 - \frac{F_z \mu}{m}(1-\lambda) + \frac{r}{J} T_b \\ \dot{v} &= -\frac{F_z \mu}{m} \end{aligned} \tag{2.3}$$

This is a nonlinear differential equation where the parameters v, μ are

time varying. Notice that the slip dynamics is scaled by the inverse of the velocity over ground of the vehicle. This will have an important effect on the control performance.
As mentioned before, the tire-road friction coefficient is itself a nonlinear function. Depending on the road condition and the tire characteristics, the peek of the friction curve will be more or less pronounced and the value of the maximum friction coefficient (μ_H) will be different. To the left of the peak the tire slip dynamics is stable. While on the right of the peak, where the slope of the curve is negative, the slip dynamics becomes unstable. The easiest way to see this is by linearizing in operating points that are in the positive respectively negative slope regions of the curve.
Another factor that is influencing the tire-road friction curve is the side-slip angle. In case of steering while free rolling, side slip together with a side force occur. This phenomenon is more pronounced in case of simultaneous braking and steering. In general, the larger the tire slip angle is the smaller the longitudinal friction will be. Naturally, this will lead to reduction of braking force when braking in a curve and consequently will increase the braking distance.

Consider the tire friction curve shown in Figure 2.2 (this curve corresponds to a high friction surface, e.g. dry asphalt). Then by fixing the braking torque T_b, one can draw the phase plane of (2.3). Figure 2.3 shows the normalized vector field of (2.3) together with some simulated solutions. The thick dashed lines represent the slip coordinate of the two equilibrium points close to the peak of the tire friction curve. These equilibrium points are on different sides of the peak (see Figure 2.2)). One of them is a stable equilibrium point $(0.079, 0)$ while the other is unstable $(0.205, 0)$. The position of these points (for a fixed curve) depends on the braking torque (T_b). It can be seen from the phase-plot that the velocity over ground dynamics is much slower than the slip dynamics. Furthermore, the slip dynamics is somewhat faster for low velocities than for high velocities. Figure 2.3 is drawn for fixed $T_b = 1300$ Nm, one can see the specific behavior of the slip dynamics, namely that for an initial slip higher than a given value (in this case 0.205), the slip dynamics becomes unstable. This would basically mean, that for a given constant braking torque $T_b = 1300$ Nm, if the point $\lambda = 0.205$ is passed, the wheel will lock.

Notice that this model is a quite simple description of the slip dy-

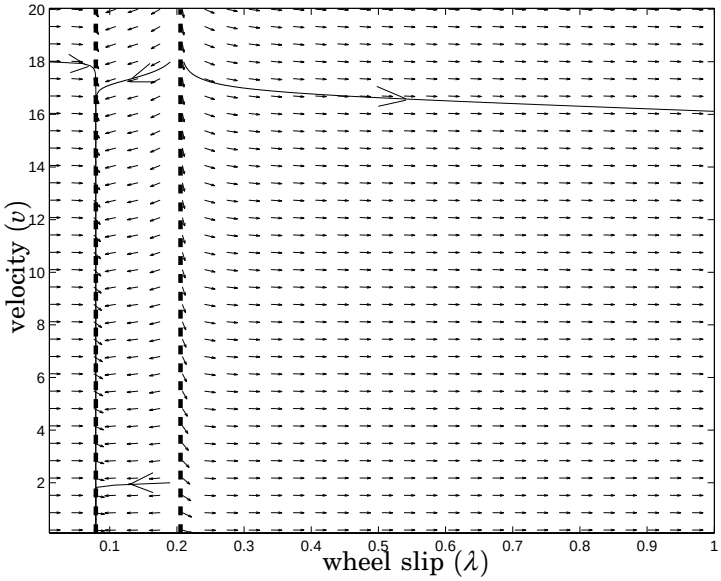

Figure 2.3 Phase plane for the quarter-car model.

namics for a wheel. It does not capture pitching motion of the car body while braking, suspension dynamics, actuator dynamics, tire dynamics nor camber angle (in the above given model, the tire is consider perpendicular on the road surface).

2.3 Existing ABS solutions

Most of ABS controllers available on the market are table and relay-feedback based, making use of hydraulic actuators to deliver the braking force [Hattwig, 1993], [Maisch *et al.*, 1993], [Maier and Müller, 1995], [Wellstead and Pettit, 1997].
The existing ABS control strategies can be divided, conceptually in two groups: wheel acceleration control and slip control. The first group of ABS use the measured angular velocity of the wheels. This control strategy is regulating the slip indirectly by controlling the wheel deceleration/acceleration. It is used mainly for hydraulic brakes with three-point-characteristics. The idea is to measure the wheel rotational velocity and compute the wheel deceleration. Then, given some thresholds for the wheel deceleration and acceleration, the pressure is increased, held or decreased preventing wheel lock during braking [Kiencke and

Nielsen, 2000]. By appropriately selecting these thresholds, the slip will oscillate around the "critical slip". This way, the friction force between the tires and the surface is close to its maximum value and the braking distance is minimized. This kind of algorithm will have as side-effect vibrations which are noticeable while braking. Todays production ABS are rule based control system, having exhaustive tables for different braking scenarios. These controllers are tuned in trial and error manner, using simulations and exhaustive field testing. The level of complexity they reach is a serious limitation for the analysis and further development of this kind of ABS. This naturally leads to model based approaches where the parameters have physical meaning. An immediate advantage for the model based controllers is that they are easier to migrate to different vehicles. In the literature another approach is presented for hydraulic brakes, where the maximum friction point is reached measuring the angular velocity of the wheel and the brake pressure [Drakunov *et al.*, 1995]. This is a model based approach and uses sliding mode to reach and track the maximum friction during emergency braking.
In [Liu and Sun, 1998], feedback linearization is used to design a slip controller and gain scheduling to handle variation with speed of the tire friction curve.

Most of the ABS control systems, including production ABS do not aim for control of tire slip at a given set-point, but they maximize the friction force between the tire and the surface by finding the peak of the friction curve. In the latest generation of brake-by-wire systems, electro-mechanic actuators are used, which are capable of delivering continuously varying and different brake force on each of the four wheels. Set-point slip is supposed to be provided by a higher level in the hierarchy (e.g. an ESP system), and can be used for stabilizing the steering dynamics of the car while braking. This way the control objective shifts to maintain a specified tire slip for each of the four wheels. This might imply different reference values for the slip of each wheel. In [Johansen *et al.*, 2001] there are presented two model based, hybrid approaches. These controllers have been tested on the same vehicle as the one used in this thesis. One of the controllers is a Lyapunov function based adaptive controller. It is using Sontag's universal formula to obtain an optimal stabilizing control law. Independently on the set-point slip, the controller also returns an estimate of the maxi-

mum friction coefficient resulting from the adaptation.
The other approach presented in [Johansen *et al.*, 2001] is a constrained LQ controller. In order to make it applicable for such fast processes, it does not rely on real-time optimization, but it evaluates the explicit solution to a suboptimal LQ problem. The controller is shown to be a piecewise linear controller. Additional gain-scheduling on tire slip and velocity is used. Test results for both approaches will be shown later, in comparison with results for the solution proposed in this thesis.

In [Jiang, 2000], different controllers have been proposed: a PID, a robust controller resulting from loop-shaping and a nonlinear PID controller. In the later the nonlinearity is a function that returns high gains for low errors and low gains for high errors. Simulation results are presented for a heavy vehicle.

2.4 The test vehicle

The test vehicle was a specially equipped Mercedes E220 passenger vehicle (see Figure 2.4). This vehicle was provided by DaimlerChrysler and it was used as test vehicle in the EU – Esprit project Heterogeneous Hybrid Control ($\mathcal{H}^2C$). It was equipped with an advanced brake-by-wire system and four state of the art electro-mechanical disk brakes.

In addition it was fitted with the following sensors:

- four wheel speed sensors,
- two accelerometers for longitudinal and lateral acceleration respectively,
- sensors for the position of the brake pedal and the force applied to the brake pedal,
- a sensor for the steering wheel angle,
- a yaw rate sensor,
- hall sensors for measuring the clamping forces at each brake.

Figure 2.4 $\mathcal{H}^2C$ test vehicle.

The ABS controllers are components of a complex brake-by-wire system. Figure 2.5 shows a block diagram of the hardware architecture of the test vehicle. It consists of four servo controllers for the brakes, a monitoring unit, a brake-by-wire control unit and a power supply unit.

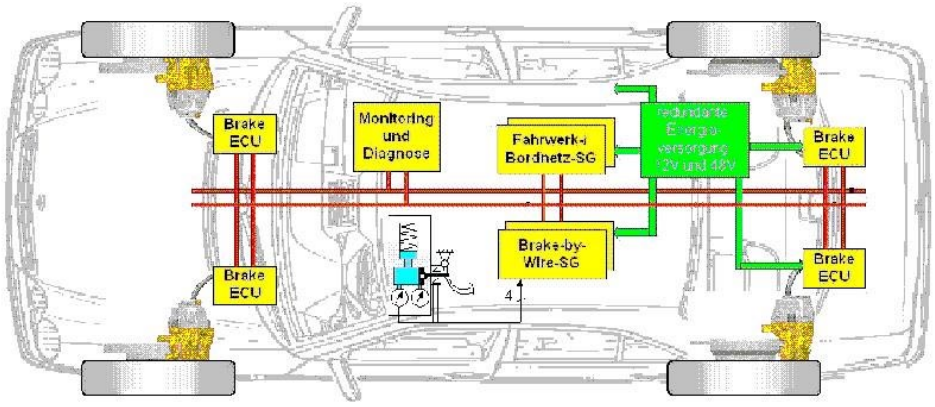

Figure 2.5 Test vehicle hardware architecture.

The electro-mechanical disk brakes are servo controlled by PID controllers. The brake-by-wire software, among other functions, gives access to sensor signals and command signals given by the ABS controllers. The modules in the above shown architecture communicate

on a synchronous TTP bus. This is advantageous from control point of view, in the sense that the time delay of the system is fixed.

2.5 The control problem

The control objective is, as mentioned above, to follow a reference trajectory for the tire slip on each of the four wheels while braking. The specifications include the following requirements [Kalkkuhl, 2001]:

- no wheel lock allowed to occur for speeds above 4 m/s
- wheel lock for a period of less than 0.2 seconds is allowed for speeds in the range of $0.8 \ldots 4$ m/s
- for speeds below 0.8 m/s the wheels are allowed to lock
- the control system should be robust with respect to other unmodeled dynamics:
  - actuator dynamics
  - suspension dynamics
- the control system should be robust to an additional time delay of 7 milliseconds due to communication

One of the most important signal in slip control is the vehicle's velocity (v). This signal is not measurable and it has to be estimated. The measured signal that is used to obtain the vehicles velocity is the tires angular velocity. Using an acceleration sensor will considerably ease this task.

In the same manner, any information about the tire friction curve has to be estimated. This later task can be challenging since the road surface conditions can change rapidly (e.g. a wet spot on a dry surface) and the estimate should converge rapidly inspite of the uncertain environment.

Thus already at this point, some of the robustness requirements can be identified due to:

- the feedback signal (λ) is not measurable but results from estimation and the signals quality is rather poor,

- time delay due to sampling and communication,
- high uncertainty in the tire-friction curve, especially in the non-linear region.

In other words it is to avoid controllers with high gains, while robustness against modeling error has to be maintained (resulting especially from the friction curve).

On the other hand fast response time is imperative, that is obviously contradictory to the above mentioned robustness requirements.

Thus, in order to have good control performance it is important to have precise estimate of the vehicles velocity, a good estimate of the surface conditions and a not too long time delay in the control system. Naturally the brake-actuator performance is also important. However, this work is focused on brake-by-wire systems equipped with electromechanical brakes, which guarantee high performance such that their limitations are not essential for the control system.

Another aim in the synthesis was to obtain a controller that is relatively easy to tune in the test vehicle and can easily be ported onto other vehicles.

As pointed out in the previous section, the proposed controller is model based, therefore a natural point to start with is the quarter car model.

2.6 Proposed design model

From the equations of motion for the quarter car, taking into account that the velocity of the car varies much slower than the other variables involved, one obtains the dynamics of the tire slip:

$$\dot{\lambda} v = -\frac{r^2 F_z}{J}\mu + \frac{r}{J}T_b \tag{2.4}$$

Relation (2.4) is a first order nonlinear differential equation due to the tire friction coefficient function. Denoting $\beta \triangleq r^2 F_z/J$, $\alpha \triangleq r/J$ and adding a time delay T, the proposed design model (see Figure 2.6) can be synthesized in the following:

$$\dot{\lambda}(t) v = -\beta\mu(\lambda(t)) + \alpha u(t-T) \tag{2.5}$$

where v is considered constant but uncertain.

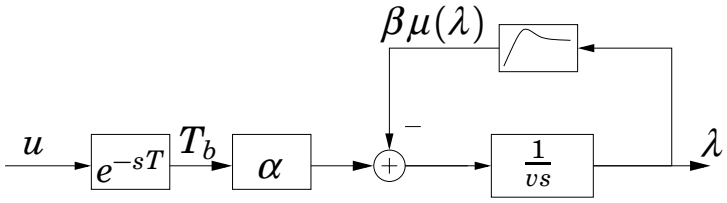

Figure 2.6 Design model for an ABS.

This model captures the main control difficulties of an anti-lock braking system. Notice that in addition to those pointed out at the beginning of this section, velocity dependence of the system is also included.

If the above presented model is linearized around an operating point, the resulting model is of the form:

$$\dot{\lambda}(t)v = -\beta(m_i\lambda(t) + \Psi) + \alpha u(t - T) \tag{2.6}$$

where m_i is the slope of the tire-friction curve at the considered operating point. Then locally the slip dynamics is given by a first order system, stable or unstable depending on the slope m_i.

Fundamental limitations

If the slope m_i resulting from the linearization is negative, one obtains locally an unstable system which in conjuncture with a time delay will give rise to fundamental limitations in control performance [Åström, 1997]. In the following a local analysis of the system in the mentioned situation will be carried out.

Consider that there are no other unstable nor non-minimum phase dynamics in the system. Then the unstable pole in question is:

$$p = \beta\frac{|m_i|}{v}$$

with $m_i < 0$. According to rules of thumb in [Åström, 1997], satisfactory control performance with a phase margin $\varphi_m = \pi/4$ requires

$$pT \leq 0.3$$

where T is the time delay, and the resulting crossover frequency is:

$$\omega_c = p\sqrt{\frac{2}{pT} - 1}$$

Consider process parameters such that $\beta \approx 440$, a time delay of $T = 14$ ms and a friction curve with local negative slope of -0.5 (that is a deflection from horizontal of -26^o). Then satisfactory control performance can be obtained until a velocity over ground not less than $v = 10$ m/s. While for a local negative slope of -0.05 (that is a deflection of approximately -3^o) the same performance can be obtained up to a velocity over ground not less than $v = 1$ m/s. The crossover frequency where this performance can be achieved being $\omega_c \approx 50$ rad/s.

Thus the time delay plays an important role in the investigated system.

2.7 Proposed control structure

As mentioned previously, many of the important signals used in the control unit are not directly measurable. The resulting control structure is of the form shown in Figure 2.7. The estimated variables are

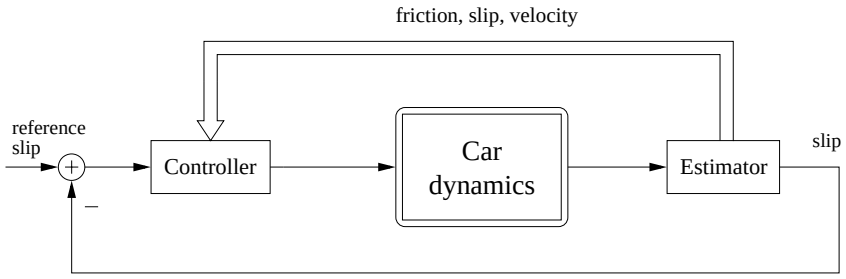

Figure 2.7 ABS control.

the tire slip (λ), velocity of the car (v) and the maximum friction coefficient (μ_H). In the design procedure these variables are considered to be measurable, i.e. no dynamics of the estimators are taken into account. This work is focused on the slip control loop based on given estimates of velocity and friction.

Due to braking the car body will exhibit a pitching motion so there is a difference between the front and back wheels behavior. On the other hand, due to the position of the center of gravity of the car there is a difference between the left and right wheels even in case of straight line braking. In the design, only a simplified model, the proposed design model (2.5) will be used. In this model none of the above mentioned phenomena are considered. The design is carried out based on the same model irrespective of the wheel location. Furthermore no suspension dynamics are explicitly considered.

Estimation

Velocity of the car is estimated using information from the acceleration sensor and the wheel speed. An extended Kalman filter is used, that besides the velocity estimates other states of the vehicle too. One of the estimated parameters is the maximum friction coefficient of the road (μ_H). However, the convergence of this estimate is slow to be effectively used for control purposes. In [Kalkkuhl *et al.*, 2000] a multiple model observer structure is proposed. This hybrid observer can be used to obtain a fast estimate of the maximum friction coefficient for the slip curve. The idea is to construct a finite set of parallel observers, each being designed for a fixed parameter value of the nonlinear plant. Defining a performance index for each of the individual observer it is possible to quantify the parameter mismatch between each of these observers and the real plant. Then, a switching logic is used to select the observer with the best performance, this way obtaining an estimate for the unknown parameter. The transient behavior for the estimate of μ_H, is much faster than the one obtained from the extended Kalman filter. In the simulations and experiments in the test vehicle, an extended Kalman filter has been used to estimate the velocity v and the multiple model observer has been used to obtain an estimate of the maximum friction coefficient μ_H.

Proposed controller

The control problem is highly uncertain and nonlinear, mainly due to the tire friction characteristics. On the other hand, fast changes in operating conditions can appear (e.g. change in surface characteristics from wet to dry road-surface). An important limiting factor is time-delay due to sampling and communication.

In the following, a synthesis method is proposed that handles uncertainties induced mainly by the friction curve, while the system has to operate in a noisy environment. A simple static model of friction is used. Based on this, we develop a gain-scheduled controller which switches between local controllers. The proposed control structure (Figure 2.8) is a gain scheduling scheme, based on tire slip value, velocity over ground (v) and the maximum friction coefficient μ_H (i.e. friction coefficient at the top of the friction curve).

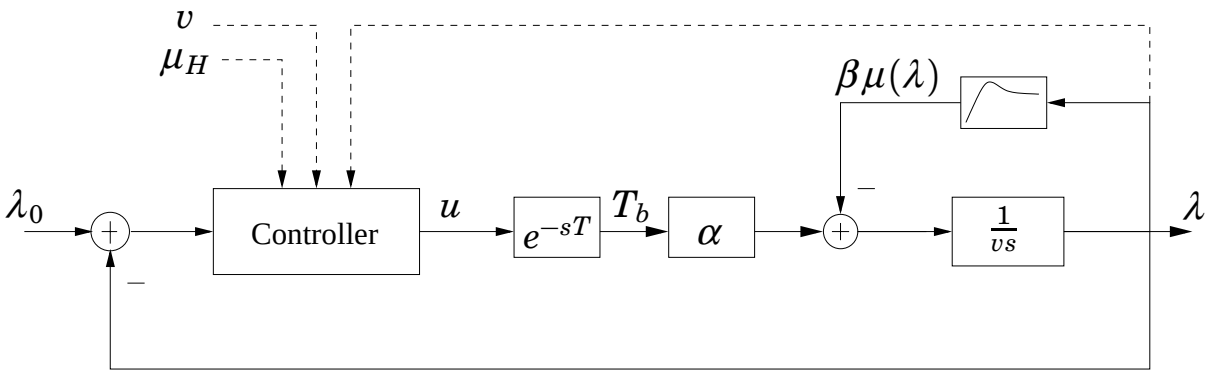

Figure 2.8 ABS control scheme.

The main idea behind the slip control design is to use a few local controllers that locally, robustly stabilize the system for different slopes of the friction curve and which tolerate the time variations due to the decreasing velocity over ground of the car (v). Switching between the local controllers is done according to the estimated friction and slip, which define the operating point on the friction curve.

Design of the local linear controllers

Due to high uncertainty in the real process, it is natural to look for a simple robust controller which can easily be tuned in the test vehicle. Therefore, PI controllers are used and the gains are scheduled based on the three variables mentioned above.

Consider a linearized model as in (2.6). The bandwidth of this model depends on v, i.e. the bandwidth is smaller for high car velocities than for low car velocities. Therefore, it is natural to design the controller to counteract this variation. The controller is scaled by

velocity (v) to ensure a higher gain for high velocities. In particular, when the system is operating at maximum friction, that is at the top of the friction curve, this scaling will theoretically remove the dependence on velocity over ground.

The chosen local controllers are of the form:

$$u(t) = k\left(\lambda_0(t) - \lambda(t)\right)v(t) + \int k_i\left(\lambda_0(t) - \lambda(t)\right)v(t)dt \tag{2.7}$$

and can be viewed as PI- controllers scaled by the velocity over ground.

As seen in (2.6), in stationarity the slip dynamics does not depend on v. Hence, in stationarity the control output should not be affected by the velocity scaling. This can be achieved by moving the velocity inside the integral, thus the integral term is kept constant as long as the slip error is zero. Also the gain k_i is inside the integral in order to obtain a smooth transition while switching between parameters [Åström and Hägglund, 1995].

Another important issue in ABS control is to prevent wheel-lock in case of changes in surface condition (e.g. a transition from dry to wet surface).A change in surface condition (e.g. transition from dry to wet surface) will act as a load disturbance of magnitude $\frac{\beta}{\alpha}(\Psi_1 - \Psi_2)$ according to (2.6). Thus, it is important that the controller minimizes the effect of load disturbances on the system. On the other hand, as seen in relation (2.6), the slope of the approximating line (resulting from the linearization of the friction curve) affects the pole of the linear system. Furthermore this is scaled by the velocity as a consequence of (2.7).

Then the local control problem is to robustly stabilize the system while minimizing the effect of load a disturbance. The main uncertainty comes from one pole and the gain of the plant.

To synthesize a PI controller that minimizes the effect of load disturbances one can solve a constrained optimization problem as suggested in [Åström *et al.*, 1998]. In order to guarantee additional robustness against the uncertainty in the plant, it is possible to add a further inequality constraint based on the circle criterion as described in [Solyom and Ingimundarson, 2002]. For improved accuracy, a model of the actuators was also introduced in the optimization.

PID controllers can be designed in the same way, with the arising design difficulties described in [Solyom and Ingimundarson, 2002].

The main potential advantage of using PID instead of PI controllers for the above described system is the ability to increase significantly the integral gain, while keeping the robustness constraints inactive. Simulations have been encouraging.

More details about the design of the local controllers are given in the next chapter, Section 3.6.

The scheduling

As described above, local robust controllers have been designed to handle different slopes on the friction curve at different velocities. By scheduling the gains k, k_i the controller can be adapted to the current operating mode/position on the estimated friction curve. In the results presented below, only two local PI controllers are used.

The choice of two local controllers is based on the observation that usually there is a maximum on the friction curve, and to the left of this there is a positive slope region , while to the right of the top (tire slip values up to 0.5 are considered) there is a region with negative slope that tends to flatten out for higher slip values. Thus it is natural to have one of the scheduling variables depending on the slip value where the assumed maximum is located (λ_H). To the left of this, a controller is used which is tuned for relatively high positive slopes, while to the right a controller that can handle negative slopes is used.

The coordinate of the maximum changes with the friction curve, thus a new scheduling variable is introduced, the maximum friction coefficient (μ_H) which is estimated. According to this a new λ_H is considered.

Due to the robustness of local designs, it is enough to use the same λ_H for a family of friction curves. This is a point where trade-off between robustness and performance will lay a mark on the controller's complexity.

Thus the scheduling scheme for the controller used in the simulations

and experiments is the following:

If *low-friction* surface
- If *low slip*$_1$ use k_1, k_{i1}
- If *high slip*$_1$ use k_2, k_{i2}

If *high-friction* surface
- If *low slip*$_2$ use k_1, k_{i1}
- If *high slip*$_2$ use k_2, k_{i2}

Notice that the same parameters k, k_i are used for low and high friction surfaces, only the scheduling based on the tire slip is changing (λ_H). This is indicated by the subscripts 1 and 2 for the scheduling slip variable. Thus this controller has seven tunable parameters.

In order to have a fast response at the beginning of the braking action, an initial braking force is applied, by initializing the controller state at once as the ABS is switched on. In this way, fast response times are possible while the controller's robustness is maintained.

2.8 Simulation and Experimental Results

The Simulation environment

The simulator contains a four wheel model including pitch dynamics of the car body. This simulation environment has been written and provided by DaimlerChrysler. Ansi C has been used as programming language for the environment. The simulator also contains the estimators for μ_H and v, that is the Multi-Model Observer and the extended Kalman filter. The control software used in the simulator is designed such that is directly transported on the platform used in the test vehicle.

Figure 2.9 shows simulation results for the left front wheel. Figures 2.12–2.14 in the Appendix show simulation results for the other wheels. As mentioned before, in the design procedure there was no information included regarding position of the wheel. Thus identical controllers are used on each of the four wheels.

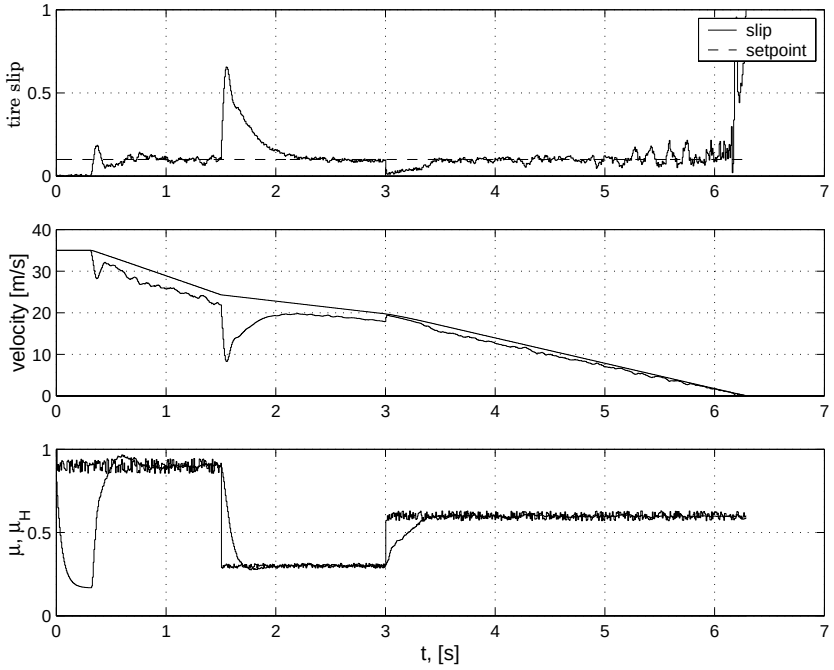

Figure 2.9 Simulation results for left front-wheel.

The first subplot shows the estimate of the controlled slip (λ) and its set-point. The second subplot depicts the vehicles velocity v (the line with negative slopes) and the wheels linear velocity ωr. The difference between this two is given by the tire slip scaled by the vehicles velocity v. The third subplot shows the estimate of the maximum friction, (denoted μ) and the maximum friction used in the simulation.

The plots show the tire slip control in a scenario where braking is commenced on a high friction surface ($\mu_H = 0.9$) then a surface with low friction is encountered ($\mu_H = 0.3$) and finally the braking is finished on a high friction surface ($\mu_H = 0.6$). That means a scenario that would simulate braking on a dry surface with a wet or icy spot.

Note the influence of the pitching dynamics which makes it harder to control the slip for the front wheel. The plot shows that in case of a change in the surface conditions, (transition from a high to a low-μ surface) the front wheels have a more pronounced tendency to lock than the rear wheels (see Figures 2.9 and 2.13). This phenomenon can be easily understood from (2.6). Pitching of the car body can be thought of as an increase of the mass acting on the front wheels, re-

spectively decrease of the mass acting on the rear wheels. The mass is proportional to the term β in (2.6). A change in the surface characteristics, will act as a load disturbance on the system, as pointed out in the previous section. This load disturbance is proportional to β, which means that a change in the surface conditions will affect much more the front wheels than the back wheels. This is exactly the behavior noticed in the simulation results.

There are also some minor differences between a left and a right wheel due to displacement in the center of gravity of the car.

The same simulations have been performed using local PID controllers. The results are presented in Figures 2.15–2.18. It can be seen that the overall performance is better.

Experimental results

The hybrid PI (HPI) controller has been tried out on the test vehicle with typical results as presented in Figures 2.10–2.21. Figure 2.10 presents the result for the left front-wheel. Here braking on dry surface with summer tires was tested. Summer tires present a prominent peek at the maximum friction coefficient, which will give rise to an unstable region for the slip dynamics.

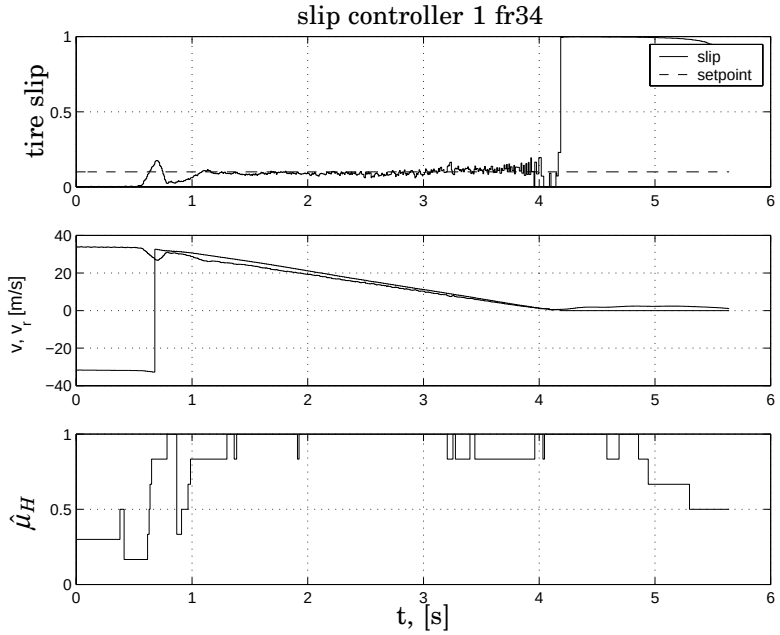

Figure 2.10 Experimental results for left front-wheel.

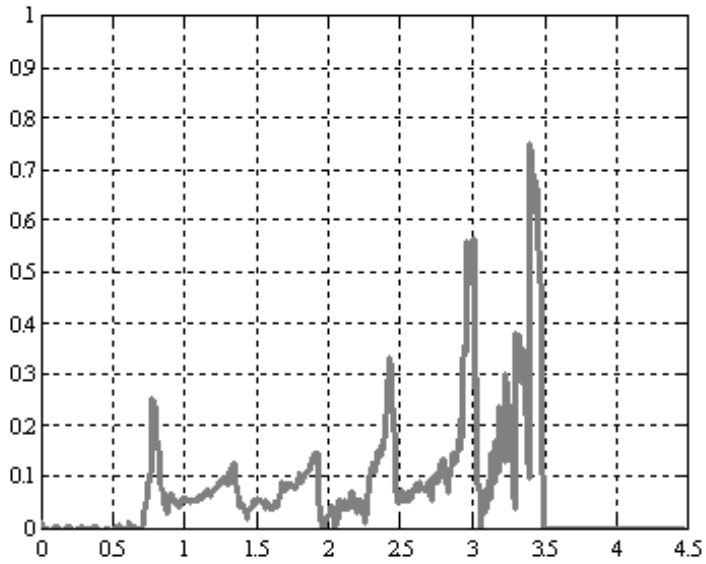

Figure 2.11 Test result for production ABS. The figure shows tire slip – time dependence.

As shown in the figure, after an initial transient the slip is controlled very smoothly. It is to be noticed that for the back-wheels the performance is even better. The initial transient is not so pronounced.

In these tests the HPI controller had the best deceleration in comparison to the approaches in [Johansen *et al.*, 2001]. The braking distance for the HPI controller, from an initial velocity of 30 m/s was between $36-41$ meters, outperforming in this sense the controllers in [Johansen *et al.*, 2001] and the production ABS.

A test result for the production ABS is shown in Figure 2.11 (the diagram depicts slip versus time dependence). As mentioned before, the production ABS was not designed to track a reference slip trajectory, but to maximize the friction force. This explain the oscillatory behavior.

For the tests as well as the simulation a gain-scheduled controller has been used with two local controllers, one for the regions with high slopes in the tire-friction curve and one for regions with low slopes in the tire-friction curve. Hence for the gain-scheduled PI controller, seven parameters have been tuned.

2.9 Conclusion

A simple but powerful design model for ABS control has been presented. Fundamental limitations on the control performance have been pointed out. A gain-scheduled PI/PID design approach has been used for the controller. Simulations and experiments in a test vehicle were performed with satisfactory results.

2.10 Appendix

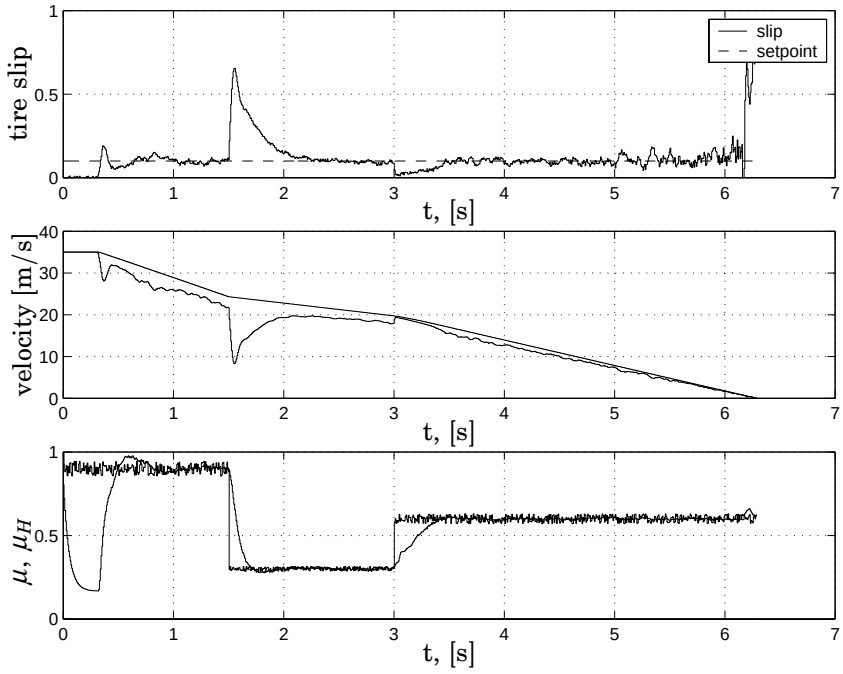

Figure 2.12 Simulation results for right front-wheel.

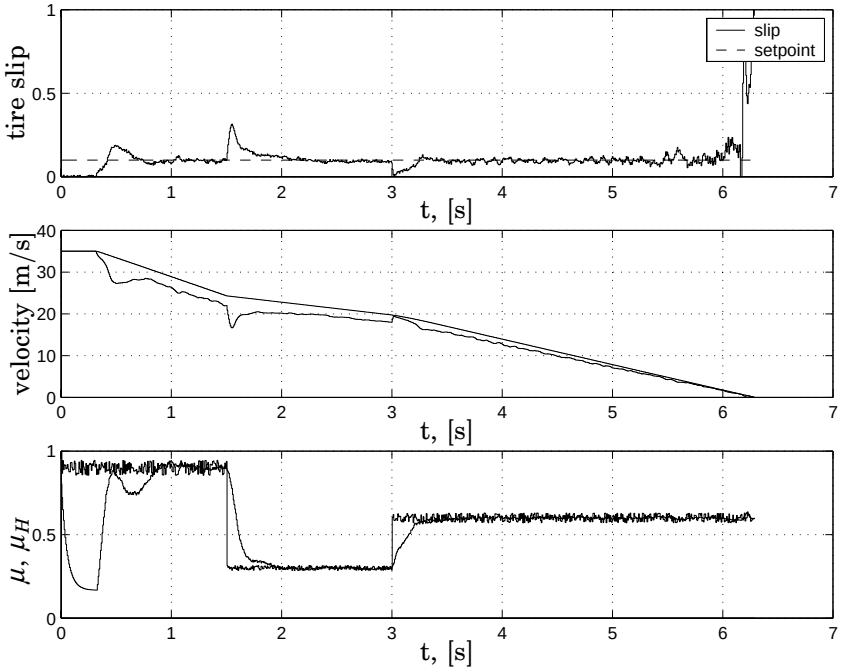

Figure 2.13 Simulation results for left back-wheel.

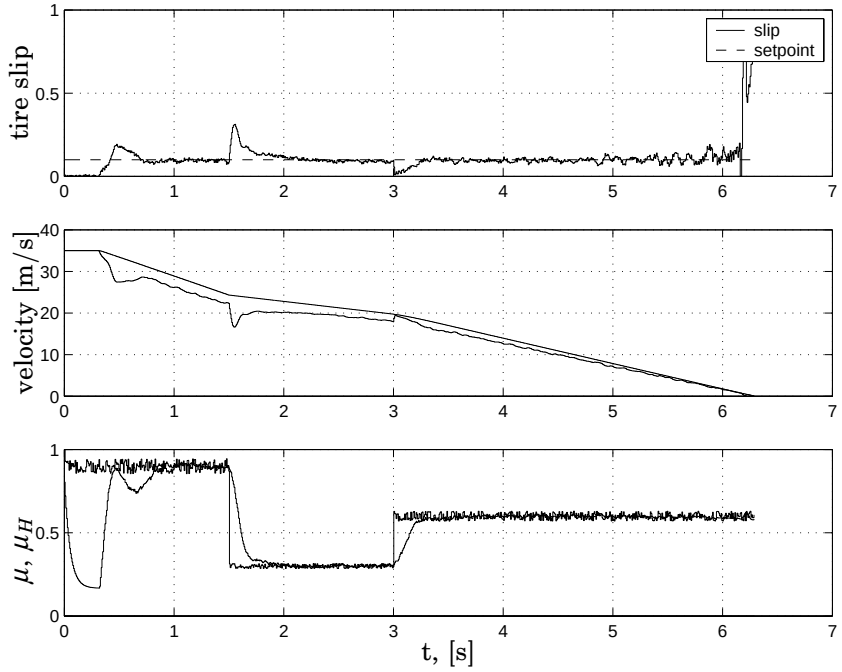

Figure 2.14 Simulation results for right back-wheel.

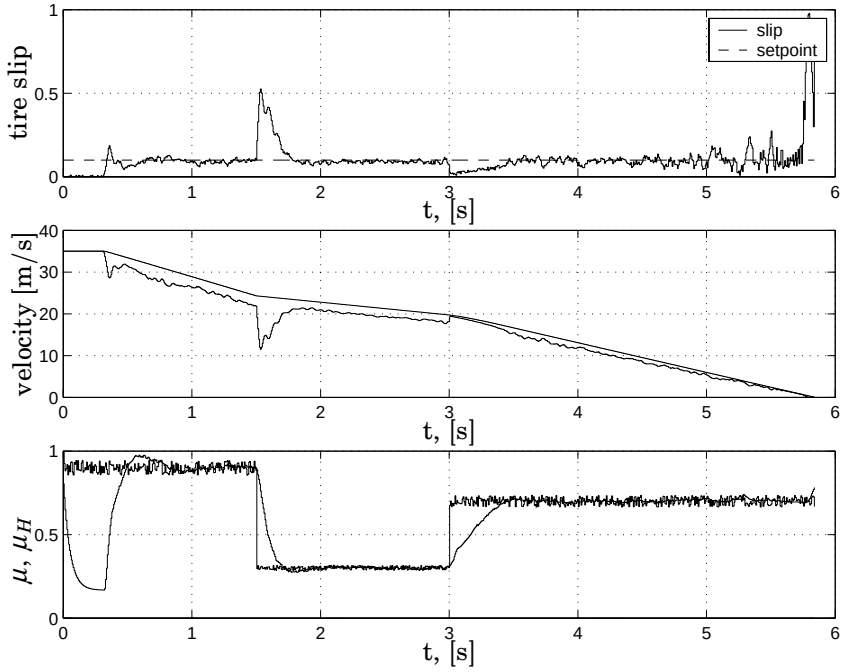

Figure 2.15 Simulation results for right front-wheel with HPID controller.

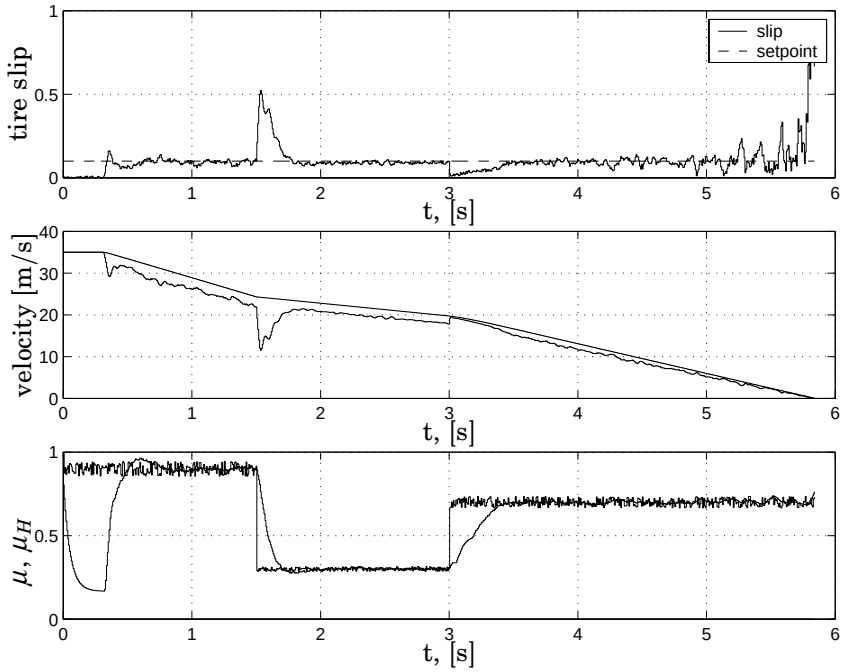

Figure 2.16 Simulation results for left front-wheel with HPID controller.

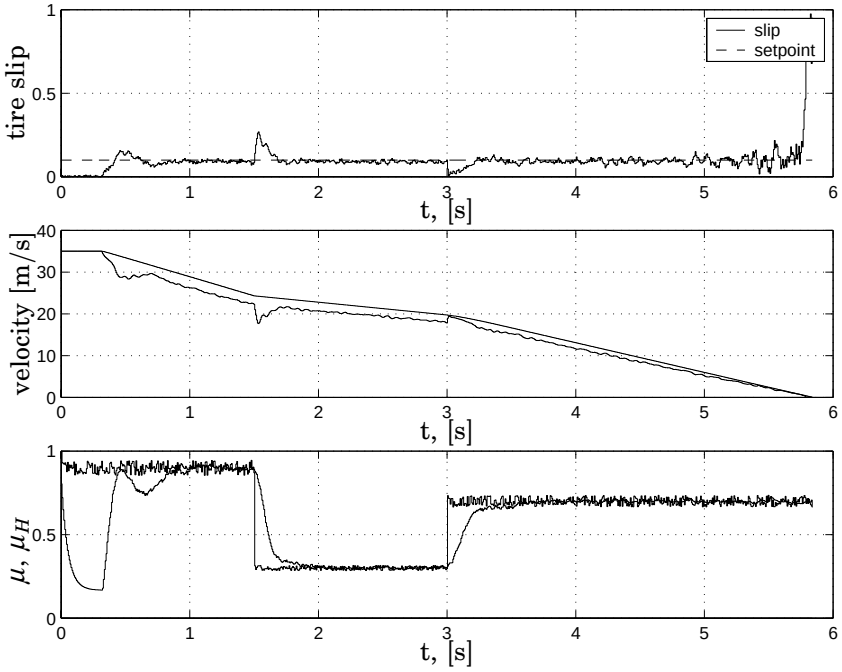

Figure 2.17 Simulation results for right back-wheel with HPID controller.

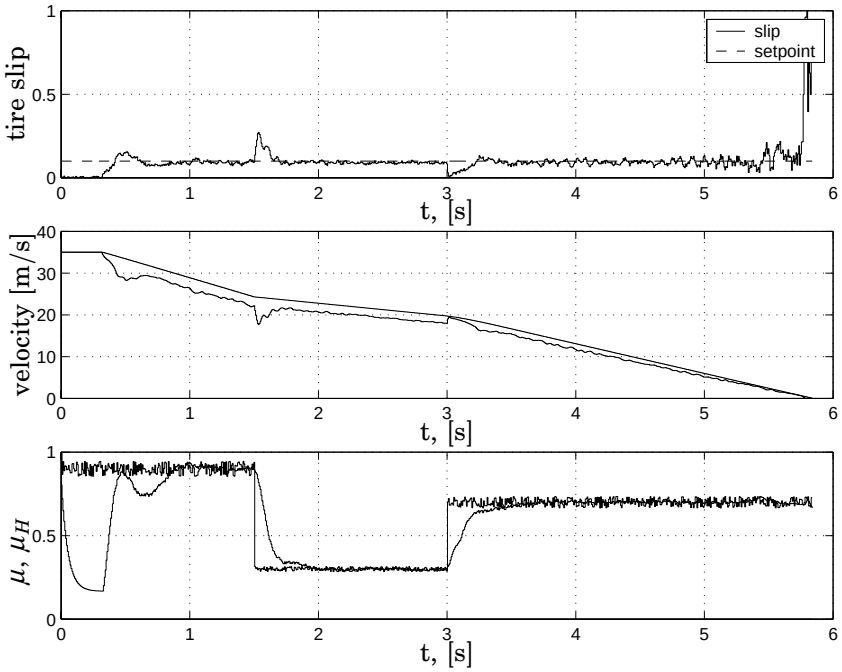

Figure 2.18 Simulation results for left back-wheel with HPID controller.

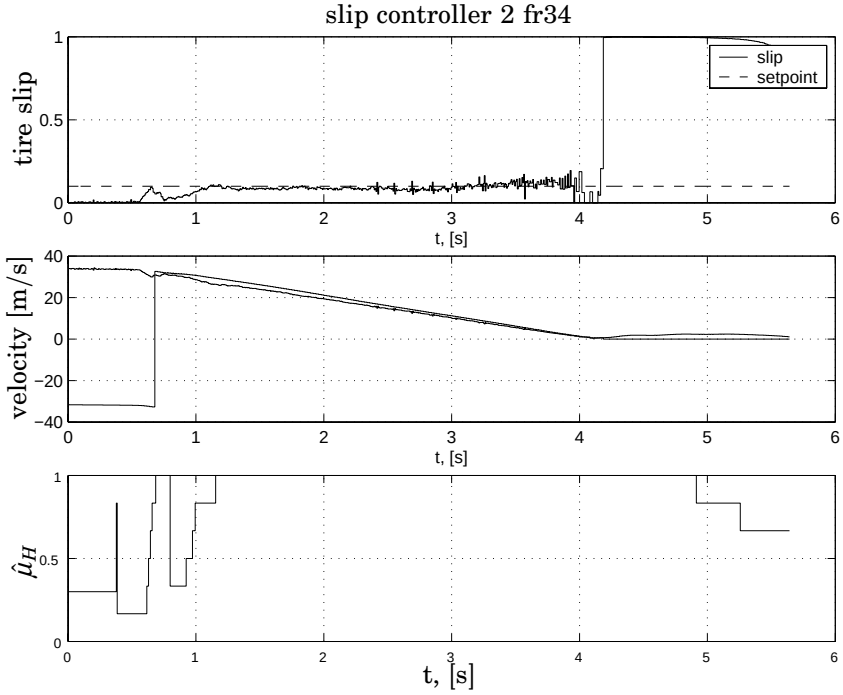

Figure 2.19 Experimental results for right front-wheel.

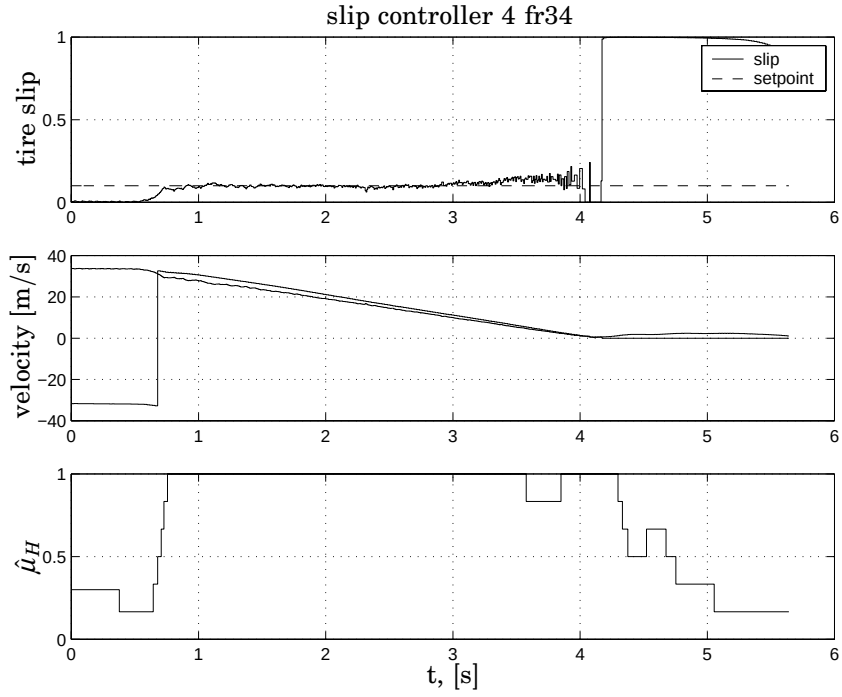

Figure 2.20 Experimental results for right back-wheel.

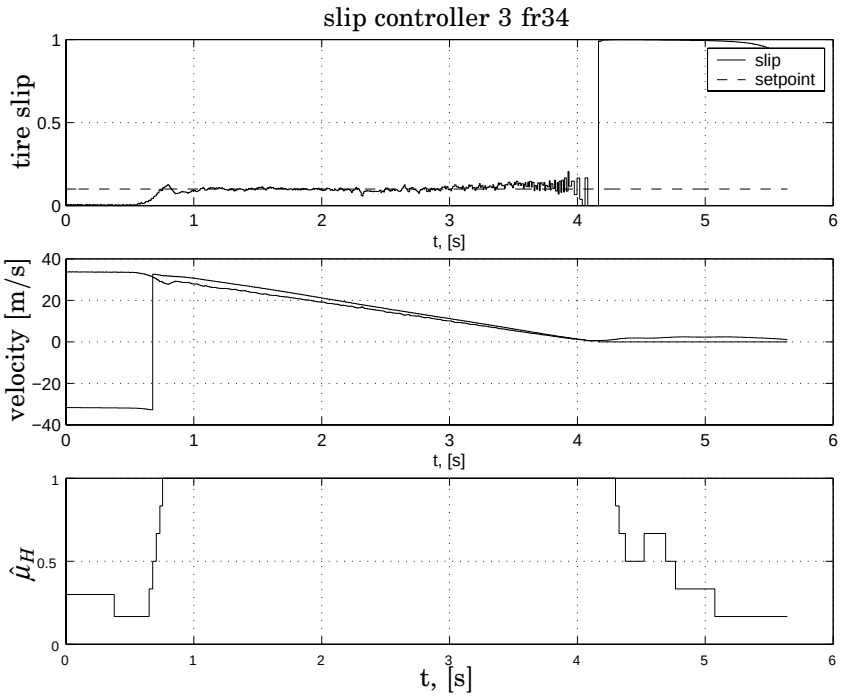

Figure 2.21 Experimental results for left back-wheel.

3

A synthesis method for robust PI(D) controllers for a class of uncertainties

3.1 Introduction

Many optimal control synthesis methods result in controllers of order related to the order of the plant. Often it is beneficial to design controllers with a restricted structure. Their performance is often close to optimal performance while they often remain substantially less complex.

One of the most common controllers is the PID controller. Its popularity is mainly due to fact that despite of its simple structure, it provides with some important functions such as: feedback, ability to eliminate steady state offsets through integral action and can anticipate the future through derivative action [Åström and Hägglund, 1995].

The synthesis procedure presented in this chapter, is an extension to synthesis procedures presented in [Åström *et al.*, 1998; Panagopoulos *et al.*, 1999] which are collected in [Panagopoulos, 2000]. There, a design procedure for PI(D) controllers was presented which minimizes the effect of a load disturbance. This is achieved by maximizing the integral gain while making sure that the closed loop system is sta-

ble. Furthermore, it is guaranteed that the Nyquist curve of the loop transfer function is outside a circle with center $-C_s$ and radius R_s. This constraint can be expressed with the equations

$$\begin{array}{ll} \text{maximize} & k_i \\ \text{subject to} & l(k,k_i,k_d,\omega) \geq R_s^2 \qquad \forall \omega > 0 \end{array} \tag{3.1}$$

where l is the function:

$$l(k,k_i,k_d,\omega) = |C_s + C(i\omega)G(i\omega)|^2 \tag{3.2}$$

and $G(s)$ is a linear time invariant plant and $C(s)$ is the PID controller parametrized as

$$C(s) = k + \frac{k_i}{s} + k_d s \tag{3.3}$$

By choosing $C_s = 1$ and R_s, the resulting controller will guarantee that the maximum of the sensitivity function equals $1/R_s$, i.e:

$$\frac{1}{R_s} = \max_{\omega} S(i\omega)$$

where $S(s) = 1/(1 + G(s)C(s))$. Controllers with constraints on the maximum complementary sensitivity function ($T(s) = 1 - S(s)$) could also be designed or a combination of these constraints. In case of PID controllers, additional inequality constraints will be added regarding the curvature and phase change of $G(s)C(s)$.

In [Panagopoulos, 2000] the main design parameter was $M_s = 1/R_s$, with values typically between 1.4–2. The value of this parameter will influence the closed loop system's damping. In the PID case, the above mentioned inequality constraints are supplemented. These will be reviewed later.

The extension presented in this chapter guarantees in addition asymptotic stability of the system when a cone bounded nonlinearity is present in feedback with part of the plant, as shown in Figure 3.1. Here, as well as in the rest of this chapter $C(s)$ represents the controller. The nonlinearity $f(\cdot,\cdot)$ is a memoryless, possibly time-varying nonlinearity within the cone given by α,$\beta \in \mathbb{R}$, $\alpha < \beta$ and $\beta \neq 0$ (see Figure 3.2), that is:

$$\alpha y^2 \leq y f(y,t) \leq \beta y^2, \;\; \forall y \in \mathbb{R}, \forall t \geq 0 \tag{3.4}$$

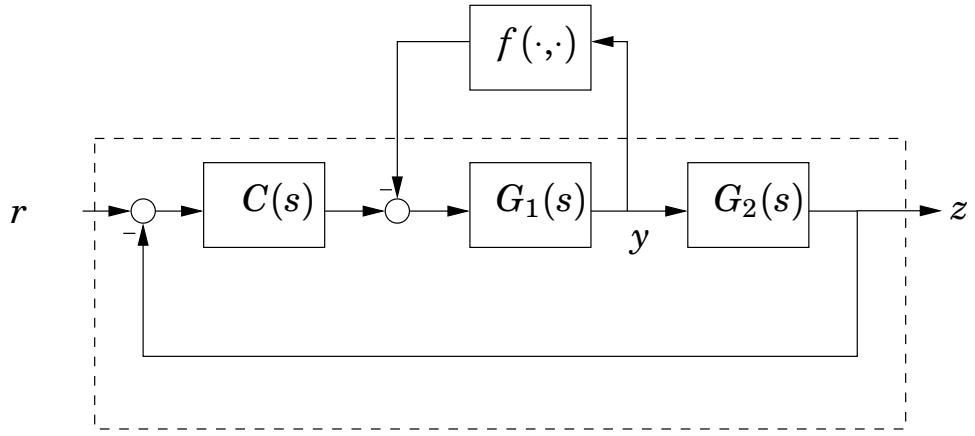

Figure 3.1 Block diagram showing nonlinearity, plant and controller.

Furthermore, it is assumed that $f(y,t)$ is piecewise continuous in t and locally Lipschitz in y. The synthesis procedure is based on a frequency domain description of the system so it is easy to take into account dead time in the plant.

The synthesis procedure can be thought of as a nonlinear optimization problem with two families of constraints. One that ensures stability and performance for the closed loop system without the nonlinearity f, and another group of constraints that will guarantee stability of the closed loop system in presence of the nonlinearity f (as

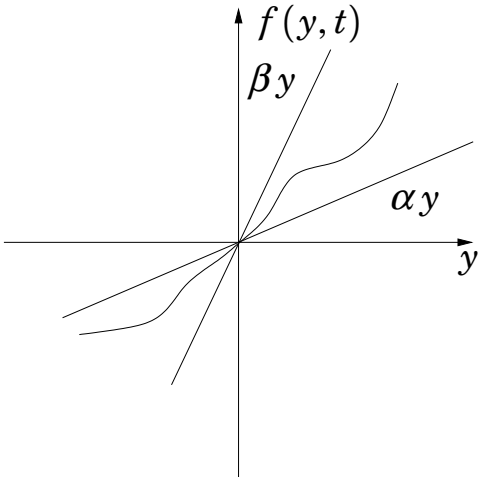

Figure 3.2 Sector bounded nonlinearity.

shown in Figure 3.1). From this point on the first family of constraints will be referred to as constraints for nominal performance, while the second group of constraints will be referred to as constraints for robust stability. Furthermore, it has to be mentioned that the constraints for nominal performance ensure robust stability against a cone-bounded nonlinearity in the control loop (see [Panagopoulos, 2000]).

The constraints for nominal performance can be considered those presented in [Panagopoulos, 2000]. This work will concentrate on the constraints for robust stability.

3.2 Sufficient conditions for stability

Consider the transfer functions $G(s)$ describing a linear plant. In feedback with a part of this plant, a cone bounded nonlinearity is present. Factorizing $G(s)$ as

$$G(s) = G_1(s)G_2(s), \tag{3.5}$$

the cone bounded nonlinearity is in feedback with $G_1(s)$, as shown in Figure 3.1. Consider for the beginning the case when the controller is a PI, i.e.:

$$C(s) = k + \frac{k_i}{s}. \tag{3.6}$$

With $G(s)$, $G_1(s)$ and $G_2(s)$ as in (3.5) define

$$P(s) \triangleq \frac{G_1(s)}{1 + C(s)G(s)} \tag{3.7}$$

Furthermore,

$$G(i\omega) = a(\omega) + ib(\omega) = r(\omega)e^{i\phi(\omega)} \tag{3.8}$$

and

$$G_1(i\omega) = a_1(\omega) + ib_1(\omega) = r_1(\omega)e^{i\phi_1(\omega)} \tag{3.9}$$

be the evaluations of the transfer functions $G(s)$, $G_1(s)$ on the positive imaginary axis.

In the case that $P(s)$ is not strictly proper, the analysis involves additional test for the well posedness of the feedback connection. For

simplicity, only the strictly proper case will be considered. Hence, a minimal realization of $P(s)$ is given by:

$$\begin{aligned} \dot{x} &= Ax + Bu \\ y &= Cx \end{aligned} \tag{3.10}$$

Then,

$$\begin{aligned} \dot{x} &= Ax - Bf(y,t) \\ y &= Cx \end{aligned} \tag{3.11}$$

describes the system in Figure 3.1 with $r = 0$.

First, some definitions will be quoted, that are necessary to state the main results.

Absolute stability [Khalil, 1992]: The system (3.11) is absolutely stable if the origin is globally uniformly asymptotically stable for any nonlinearity in the given sector. It is absolutely stable with a finite domain if the origin is uniformly asymptotically stable.

Positive real transfer function [Slotine and Li, 1991]: A transfer function $H(s)$ is positive real (PR) if

$$\mathrm{Re}\{H(s)\} \geq 0, \ \forall \mathrm{Re}\{s\} \geq 0.$$

It is strictly positive real (SPR) if $H(s-\varepsilon)$ is positive real for some $\varepsilon > 0$.

It is a well known result that a transfer function $H(s)$ is SPR if and only if $H(s)$ is Hurwitz and

$$\mathrm{Re}\{H(j\omega)\} > 0, \ \forall \omega \geq 0$$

Conditions for absolute stability of system (3.11) can be obtained by applying the circle criterion, for the transfer function $P(s)$ as it is connected in a loop with the nonlinearity. Therefore the circle criterion for a scalar plant will be cited:

PROPOSITION 3.1—CIRCLE CRITERION [KHALIL, 1992]
Consider the system (3.11), where (A, B) is controllable, (A, C) is observable. $f(y,t)$ is locally Lipschitz in y, piecewise continuous in t and satisfies the sector condition (3.4) globally. Then, the system is absolutely stable if $A - \alpha BC$ is Hurwitz and

$$\frac{1+\beta P(s)}{1+\alpha P(s)}$$

is strictly positive real. □

In order to state the main results, some intermediary steps will be helpful.

LEMMA 3.1
Consider $P(s)$ as in (3.7) and $\alpha, \beta \in \mathbb{R}$. Then $\forall \omega > 0$

$$\mathrm{Re}\left\{\frac{1+\beta P(j\omega)}{1+\alpha P(j\omega)}\right\} > 0 \tag{3.12}$$

if and only if

$$r(\omega)^2 k^2 + p(\omega)k + \frac{r(\omega)^2}{\omega^2}k_i^2 + q(\omega)k_i + h(\omega) > 0 \tag{3.13}$$

with

$$\begin{aligned} p(\omega) &= (a(\omega)a_1(\omega) + b(\omega)b_1(\omega))(\alpha+\beta) + 2a(\omega) \\ q(\omega) &= \frac{1}{\omega}\left((a(\omega)b_1(\omega) - b(\omega)a_1(\omega))(\alpha+\beta) + 2b(\omega)\right) \\ h(\omega) &= (\alpha+\beta)a_1(\omega) + \alpha\beta r_1(\omega)^2 + 1 \end{aligned} \tag{3.14}$$

□

The proof of this lemma is based on elementary but tedious computations and it can be found in the Appendix of this chapter.

Lemma 3.1 states that since in the control structure (3.7) the controller $C(s)$ is a PI, the positivity constraint (3.12) can be checked in the controller's parameter space, i.e. $k - k_i$ plane. The parametric curve

in (3.13) is an ellipse in the $k - k_i$ plane, for a given frequency ω. This result is similar to those in [Åström *et al.*, 1998; Panagopoulos *et al.*, 1999; Saeki and Kimura, 1997].

Based on the circle criterion and the lemma above, the following theorem for absolute stability of system (3.11) can be stated:

THEOREM 3.1
Let A,B,C describe a minimal realisation of the system defined by (3.5)−(3.9). Consider $\alpha, \beta \in \mathbb{R}$ and a function $f(y,t)$ piecewise continuous in t and locally Lipschitz in y such that (3.4) holds.
If $A-\alpha BC$ is Hurwitz and (3.13) holds then the system of form (3.11) is absolutely stable.

□

Proof:
The circle criterion provides sufficient conditions for absolute stability of the system. The only condition left to prove is that $\frac{1+\beta P(s)}{1+\alpha P(s)}$ is SPR. All poles of $\frac{1+\beta P(s)}{1+\alpha P(s)}$ have strictly negative real part due to the fact that $A - \alpha BC$ is Hurwitz. By Lemma 3.1, $\forall \omega > 0$

$$\mathrm{Re}\left\{\frac{1+\beta P(j\omega)}{1+\alpha P(j\omega)}\right\} > 0$$

is equivalent to (3.13), and since $P(0) = 0$ the proof is complete. ◇

This result is equivalent to that presented in [Solyom and Ingimundarson, 2002]. The conditions presented here have a higher degree of generality while the parametric relations are simpler.

In many engineering applications it is of interest to look at other equilibrium points than the origin. This is natural since often the equilibrium point will change depending on the systems input. Obviously any equilibrium point can be analyzed by shifting it to the origin. This would mean different tests for each equilibrium point. Therefore it is of special interest to derive a single test, that will give information about the stability of equilibrium points depending on the input signal. In this sense the following theorem gives useful result.

THEOREM 3.2
Consider the system:

$$\begin{aligned} \dot{x} &= Ax - Bw + B_r r \\ w &= f(Cx) \end{aligned} \tag{3.15}$$

with (A, B), (A, C) controllable respectively observable pairs and f a continuous, memoryless scalar nonlinearity. Denote $P(s) = C(sI - A)^{-1}B$.
If there exist $\alpha, \beta \in \mathbb{R}$ such that

$$\alpha \leq \frac{f(y_1) - f(y_2)}{y_1 - y_2} \leq \beta, \quad \forall y_1, y_2 \in \mathbb{R}, \tag{3.16}$$

$$\text{Re}\left\{ \frac{1 + \beta P(j\omega)}{1 + \alpha P(j\omega)} \right\} > 0, \quad \forall \omega \geq 0 \tag{3.17}$$

and $A - \alpha BC$ is Hurwitz then every equilibrium point of (3.15) corresponding to some constant r, is a global uniformly asymptotically stable equilibrium point. □

Proof:
Consider the change of variable: $\xi = x - x_r$ with x_r given by

$$0 = Ax_r - Bf(Cx_r) + B_r r$$

for some constant r. If for a fixed r, the solution of the above equation exists, then it is unique. (See Lemma 3.2 in the Appendix.)

Consider the system:

$$\dot{\xi} = A\xi - B\varphi(C\xi)$$

with the new nonlinearity $\varphi(C\xi) = f\left(C(\xi + x_r)\right) - f(Cx_r)$. According to (3.16) this is a cone bounded nonlinearity.
Using the circle criterion for this system, it can be concluded that $\xi = 0$ is a global uniformly asymptotically stable equilibrium point. Hence x_r is a global uniformly asymptotically stable equilibrium point of (3.15), for the considered $r \in \mathbb{R}$. ◇

Consider now the sytem defined by (3.5) − (3.9) in feedback with a nonlinearity f. This system is shown in Figure 3.1. The system equations are given by:

$$\begin{aligned} \dot{x} &= Ax - Bf(y) + B_r r \\ y &= Cx \\ z &= C_r x \end{aligned} \tag{3.18}$$

where (A, B), (A, C) are controllable respectively observable pairs and f is a continuous, memoryless scalar nonlinearity. This system has a special structure, in the sense that it uses a PI controller. The problem is to investigate the equilibrium points with respect to r. Hence, for system (3.18) Theorem 3.2 can be applied. Since the controller is a PI, the positivity condition (3.17) can be checked, according to Lemma 3.1, in the parameter space of the controller ($k - k_i$ plane). Then the following proposition can summarize the result for the case of PI controllers.

PROPOSITION 3.2
Let A,B,C describe a minimal realisation of the system defined by (3.5)−(3.9). If there exist $\alpha, \beta \in \mathbb{R}$ such that (3.13), (3.16) hold and $A - \alpha BC$ is Hurwitz then every equilibrium point of (3.18) corresponding some constant r, is a global uniformly asymptotically stable equilibrium point. □

Thus in the case of PI controllers, the constraints that guarantees nominal performance, robust stability as well as solution for the servo problem in case of a constant input can be easily drawn in the controller's parameter space (k–k_i plane). In this way the optimization problem of finding the maximum k_i such that these constraints hold can be solved by visual inspection.

3.3 Other design issues

PID controllers

In case of PID controllers the synthesis procedure is similar to the PI case presented above. The above presented results hold with minor changes. The easiest way to migrate the results to the case of PID controllers is by replacing the parameter k_i with $k_i - \omega^2 k_d$. This way the parameter space becomes three dimensional (k, k_i, k_d) making the synthesis procedure more complex.

Furthermore, in the case of PID controllers it was found in [Panagopoulos, 2000] that the sensitivity constraint alone was not sufficient to guarantee a nice, well-damped response. Condition ensuring negative curvature of the loop gain and the monotonicity of the phase function of the loop gain were added to the optimization problem. In the case of integrating processes only the second condition is imposed.

Thus in contrary to the PI case, where the optimization problem could be easily solved by visual inspection, for the case of PID controllers a similar approach is significantly more difficult. Therefore an optimization routine is more adequate to solve this problem.

3.4 Optimization

Using the results presented in the previous section the synthesis problem can be stated as the following optimization problem.

$$\begin{aligned} \max \quad & k_i & & \\ \text{subject to} \quad & f(k, k_i, k_d, \omega_1) \geq R_s^2 & \forall \omega_1 > 0 & \quad (3.19) \\ & g(k, k_i, k_d, \omega_2) \geq 0 & \forall \omega_2 > 0 & \quad (3.20) \\ & k > 0, k_i > 0, k_d > 0 & & \quad (3.21) \end{aligned}$$

Constraint (3.21) guarantees that the controller will not have an unstable zero. The two frequency dependent inequalities define the exterior of two ellipses for a fixed frequency. For $0 < \omega < \infty$ these ellipses generate envelopes that define the boundaries of the set of parameters which satisfy the constraints.

The constraints can be visualized by plotting the ellipses for a tight griding of frequencies, enabling to visually identify the optimizer. This graphical approach is suitable when PI design is considered but is more difficult in case of PID controllers. However it is possible to plot the ellipses for a grid of k_d values. Here is of more interest to have a numerical optimization procedure that can give the desired result. For most numerical optimization procedures it is important to have good starting values. The problem of finding good starting values is related to determining if the problem has any feasible solution. But a quick view of the constraints for a few values of k_d should be sufficient to obtain good starting values and see if the problem is feasible.

Automating the synthesis procedure

So far the synthesis procedure that has been presented would need much manual intervention. It is of interest to automate the synthesis procedure so that only the process and the parameters characterizing the uncertainties would need to be specified. This is in principle to automate the checking of feasibility and finding a good start value for the numerical optimization procedure. For ideas about this issue see [Panagopoulos, 2000].

3.5 Examples

Two examples of PI controller design will now be given followed by one example for PID design.

EXAMPLE 3.1
Consider the system in Figure 3.1 with

$$G_1(s) = \frac{1}{(s+1)^3} \qquad G_2(s) = 1$$

and a static, time varying nonlinearity $f(y_1, t) : \alpha \leq f(y,t)/y \leq \beta$ with $\alpha = 1$, $\beta = 4$. In particular if the cone bounded uncertainty would be an uncertain gain the transfer function would be given by $G(s) = \frac{1}{(s+1)^3+\Delta}$ where $\Delta \in [1, 4]$. The two constraints, equations (3.19) and (3.20), will give rise to constraint surfaces as shown in Figure 3.3. As seen in the figure, in this case, the optimizer considering the

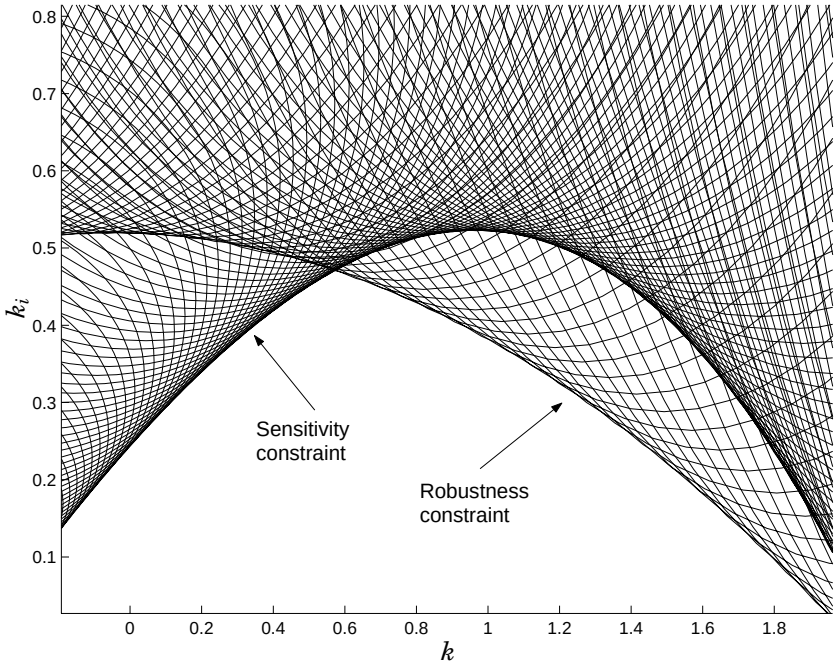

Figure 3.3 Constraints in the k-k_i plane in Example 3.1.

stability constraints for the linear system (in the figure indicated as "sensitivity constraint") will not guarantee stability of the nonlinear system with cone bounded uncertainty as considered above. The stability constraint for the nonlinear system is indicated in the figure as "robustness constraint". Choosing the maximum k_i that falls below both constraint surfaces and a corresponding k, Theorem 3.1 guarantees absolute stability of the nonlinear system.

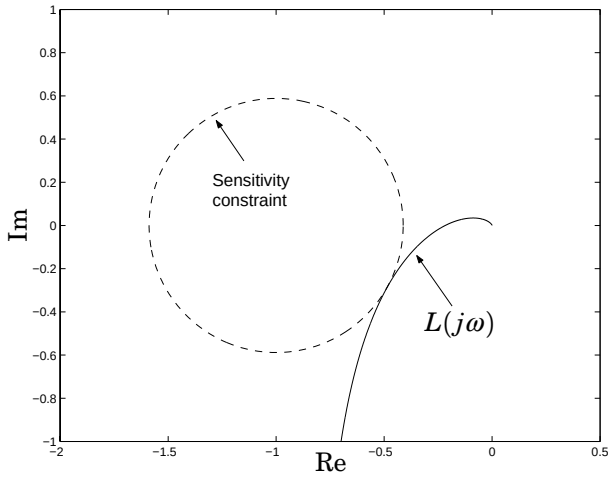

Figure 3.4 Nyquist plot of the loop transfer function $L(s)$ in Example 3.1.

The Nyquist plot of the loop transfer function and the transfer function defined by equation (3.7), shown in the Figures 3.4 respectively 3.5, confirm that the constraints are not violated. □

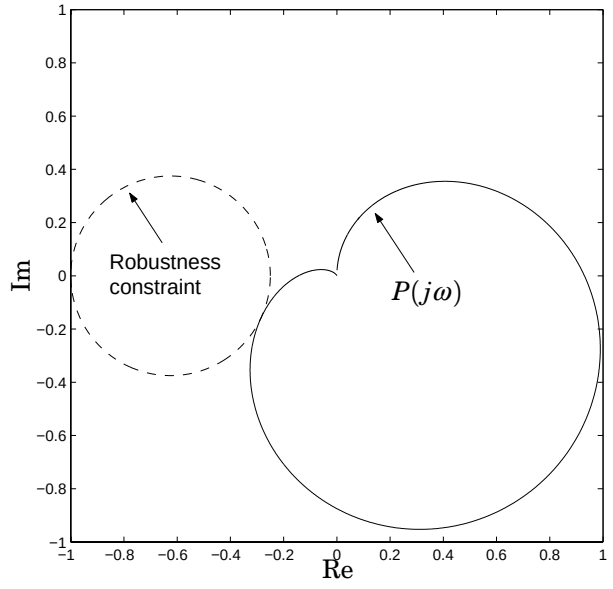

Figure 3.5 Nyquist plot of $P(s)$ in Example 3.1.

EXAMPLE 3.2
Consider the system in Figure 3.1 with

$$G_1(s) = \frac{1}{s+1} \qquad G_2 = e^{-0.1s}$$

and a static, time varying nonlinearity $f(y,t) : \alpha \leq f(y,t)/y \leq \beta$ with $\alpha = -5,\ \beta = 5$. In particular, if $f(y,t)$ is an uncertain gain, the transfer function would be given by: $G_1(s) = \frac{1}{s+\Delta}e^{-0.1s}$ where $\Delta \in [-4, 6]$. Constraints (3.19) and (3.20) give rise to constraint surfaces as shown in Figure 3.6. From this figure results that neither in this case the "op-

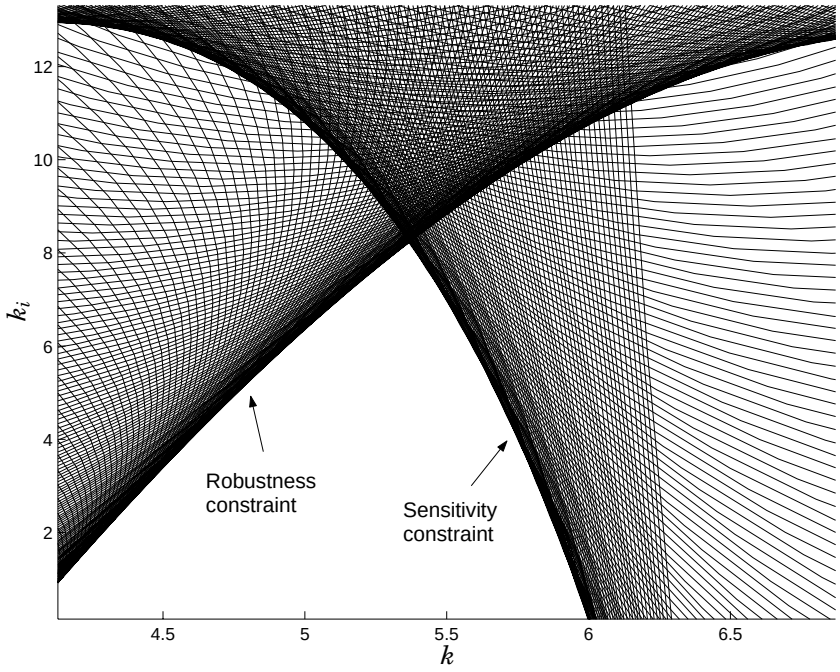

Figure 3.6 Constraints in the k–k_i plane in Example 3.2.

timum", considering only the stability constraints for the linear system, will guarantee stability of the nonlinear system. Choosing the maximum k_i that falls below both constraint surfaces and a corresponding k, Theorem 3.1 guarantees absolute stability of the nonlinear system.

The Nyquist plot of the loop transfer function and (3.7), shown in Figure 3.7 respectively 3.8, confirm that the constraints are not violated.

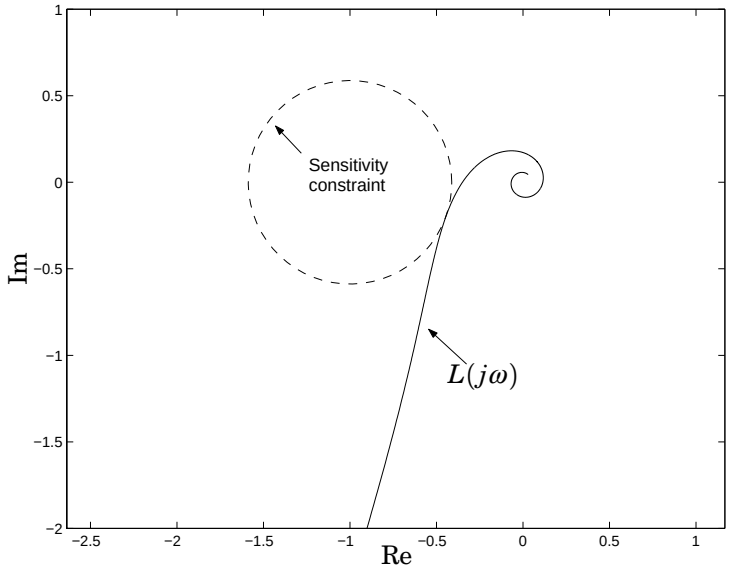

Figure 3.7 Nyquist plot of the loop transfer function $L(s)$ in Example 3.2.

Consider now, $f(y,t)$ such that its slope at the equilibrium point, is $\alpha = -5$. Theorem 3.2 guarantees stability for this equilibrium point too. □

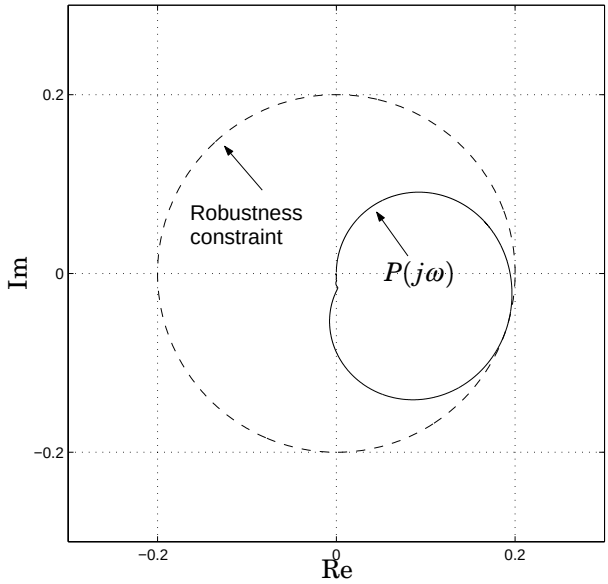

Figure 3.8 Nyquist plot of $P(s)$ in Example 3.2.

EXAMPLE 3.3
Assume a PID controller is wanted for the process in Example (3.2). The maximum integral gain was $k_i = 8.0$ when only a PI controller was used. By plotting the ellipses for a selection of k_d values the following solution could be obtained.

$$[k\ k_i\ k_d] = [6.7\ 22.5\ 0.2]$$

The envelopes that the ellipses generated for these parameters can be seen in Figure 3.9. A substantial increase in integral gain could be achieved with the PID design. The process on the other hand is simple so this could be expected.

The Nyquist plot of the loop transfer function and (3.7), shown in Figure 3.10 respectively 3.11, confirm that the constraints are not violated.

Notice that the constraints shown in Figure 3.9 do not contain any extra constraints on the curvature nor the phase lead of the loop transfer function as suggested in Section 3.3. However, in this case, the Nyquist curve of the loop transfer function ($L(j\omega)$) has a satisfactory

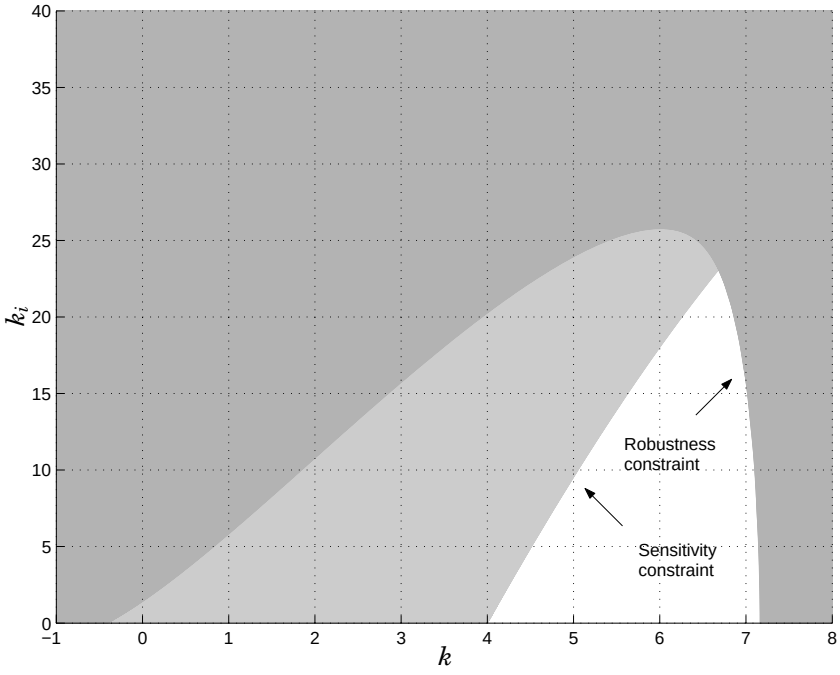

Figure 3.9 Ellipses for $k_d = 0.2$ in Example 3.3.

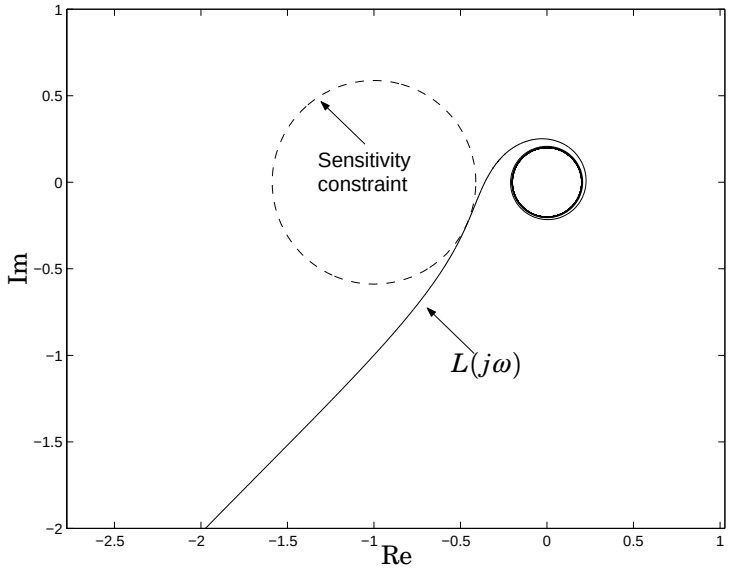

Figure 3.10 Nyquist plot of the loop transfer function $L(s)$ in Example 3.3.

behaviour. Naturally, for more complicated systems this might not be the case. □

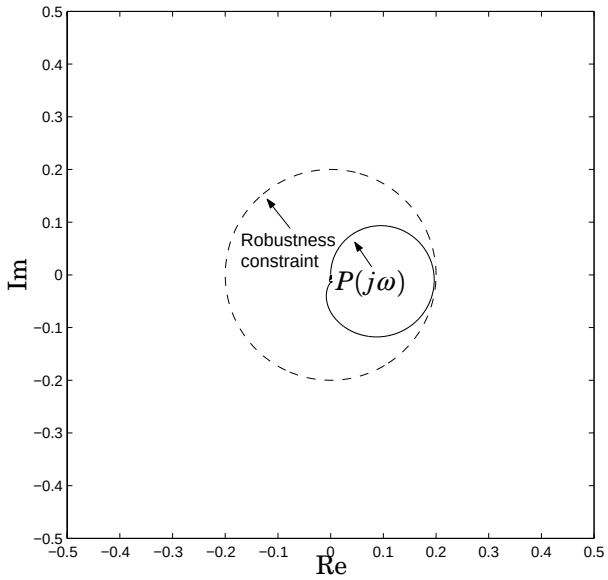

Figure 3.11 Nyquist plot of $P(s)$ in Example 3.3.

3.6 Controller Synthesis for an Anti-lock Braking System

In this section an application of the above described synthesis method to an Anti-lock Braking System (ABS) will be presented. The synthesis method will be used to design local PI(D) controllers for a gain scheduled scheme as presented in Chapter 2 and [Solyom and Rantzer, 2002a]. The proposed design model from chapter one will be used to design the local controllers.

According to (2.5) the plant can be written as:

$$\dot{\lambda}(t)v = -\beta\mu(\lambda(t)) + \alpha u(t-T)$$

As pointed out before $\mu(\lambda)$ is a nonlinear function of λ, and possibly time varying (e.g. as result of a change in surface conditions). Moreover, v is the car's traveling velocity, which is obviously time varying however it has a slower dynamics than the tire slip λ.

The tire friction curve, $\mu(\lambda)$, is highly uncertain. It depends on many variables, as described in Chapter 2. However, it is safe to assume that is cone bounded. Furthermore we assume that is locally Lipschitz in λ. Then theorems 3.1 and 3.2 can be used to design optimal controllers that are robust against a cone bounded nonlinearity, which in this case is the tire friction curve.

Applying the synthesis method for a cone that contains the entire friction curve will give rise to difficulties. In case that all equilibrium points are considered (Theorem 3.2) it is very likely that the optimization problem turns out infeasible. This can be due to a potentially large cone while the degrees of freedom in the controller are restricted. On the other hand, as pointed out in Section 2.6, limitations on the control performance arise due to time delay and unstable dynamics. Even if it would be possible to stabilize the system in any point on the entire friction curve, the resulting controller would be very conservative and it would not satisfy the performance requirements on the ABS.

A way around this problem is to design controllers for different smaller cones and then switch between them according to some scheduling variables. These cones are supposed to describe different regions of a typical friction curve. Using Theorem 3.2, one would look at regions on the friction curve with slopes in a given cone. The resulting

controllers will stabilize any equilibrium point on the considered cone bounded nonlinearity. Considering all possible slopes of the friction curves, by Theorem 3.2 one is able to stabilize any point on a friction curve by its appropriate controller. Then by switching between these controllers, it will be possible to stabilize points on any friction curve that are contained in the considered cone and has its slope confined to the same cone.

The scheduling variable is supposed to be able to determine the operating point on the friction curve. This was presented in Chapter 2 of this work.

Furthermore, scaling the controller by velocity over ground (v) as suggested in Section 2.7, will in turn scale the relative uncertainty caused by the friction curve by v^{-1}. This scaled uncertainty remains in feedback with a nominal plant as shown in Figure 2.6. Considering the uncertainty as being cone bounded, this scaling will "tighten" the cone with increasing velocity.

As pointed out in Section 2.7, to prevent wheel lock in case of sudden change in the surface conditions, it is important that the controller minimizes the effect of load disturbances.

Thus the synthesis methods proposed in this chapter can be directly applied to this problem, resulting in optimal controllers that stabilize the system for a family of friction curves.

Furthermore, to obtain a better performance, the actuator dynamics have been also considered. These are incorporated in $G_2(s)$ and can be easily handled by the proposed design method.

It is worth mentioning that during the field tests, diagrams of the kind shown in Figure 3.3, showing the constraint surfaces in the k–k_i plane, has been proven to be helpful in retuning the controllers.

3.7 Conclusions

The synthesis method presented deals with design of robust controllers with restricted structure, in particular PID controllers. The uncertainty in the plant is described by a cone bounded nonlinearity, which is in feedback with part of the plant. To obtain a "good" controller, maximum sensitivity is limited as well. The synthesis method presented requires much manual intervention but it is the believe of the author

it can be automated significantly. The design method was successfully used to tune local controllers for an Anti-lock Braking System.

3.8 Appendix

Proof of Lemma 3.1:

$$\begin{aligned}
&\mathrm{Re}\left\{\frac{1+\beta P(s)}{1+\alpha P(s)}\right\} = \mathrm{Re}\left\{\frac{1+C(s)G(s)+\beta G_1(s)}{1+C(s)G(s)+\alpha G_1(s)}\right\} \\
&\mathrm{Re}\left\{\frac{1+(k-j\frac{k_i}{\omega})(a(\omega)+jb(\omega))+\beta(a_1(\omega)+jb_1(\omega))}{1+(k-j\frac{k_i}{\omega})(a(\omega)+jb(\omega))+\alpha(a_1(\omega)+jb_1(\omega))}\right\} > 0 \iff \\
&\mathrm{Re}\left\{\left(1+\left(k-j\frac{k_i}{\omega}\right)(a(\omega)+jb(\omega))+\beta(a_1(\omega)+jb_1(\omega))\right)\right. \\
&\qquad \left.\left(1+\left(k+j\frac{k_i}{\omega}\right)(a(\omega)-jb(\omega))+\alpha(a_1(\omega)-jb_1(\omega))\right)\right\} > 0
\end{aligned} \tag{3.22}$$

which represents a region outside some ellipses (depending on ω) in the $k-k_i$. By identifying the coefficients of k and k_i in (3.22), one obtains inequality (3.13) with parameters as in (3.14). ◇

LEMMA 3.2
Consider the system:

$$\begin{aligned}
\dot{x} &= Ax - Bw + B_r r \\
w &= f(Cx)
\end{aligned} \tag{3.23}$$

with A Hurwitz, (A,B), (A,C) controllable respectively observable pairs and f a continuous, memoryless scalar nonlinearity. Denote $P(s) = C(sI-A)^{-1}B$.
Assume that there exist $\alpha, \beta \in \mathbb{R}$ such that

$$\alpha \leq \frac{f(y_1)-f(y_2)}{y_1-y_2} \leq \beta, \quad \forall y_1, y_2 \in \mathbb{R},$$

$$\mathrm{Re}\left\{\frac{1+\beta P(j\omega)}{1+\alpha P(j\omega)}\right\} > 0, \quad \forall \omega \geq 0. \tag{3.24}$$

If for a given $r_0 \in \mathbb{R}$, (3.23) has an equilibrium point then it is unique. □

Proof
An equilibrium point x_e corresponding an $r_0 \in \mathbb{R}$ satisfies the equation:

$$0 = Ax_e - Bf(Cx_e) + B_r r_0 \tag{3.25}$$

Assume there exist $x_{e1} \neq x_{e2}$ satisfying (3.25) for the same r_0. Since A is Hurwitz, one obtains:

$$x_{ei} = A^{-1}Bf(Cx_{ei}) - A^{-1}B_r r_0, \quad i = 1, 2$$

then

$$x_{e1} - x_{e2} = A^{-1}B(f(Cx_{e1}) - f(Cx_{e2}))$$

hence

$$\alpha \leq \frac{f(Cx_{e1}) - f(Cx_{e2})}{Cx_{e1} - Cx_{e2}} = \frac{1}{CA^{-1}B} \leq \beta \tag{3.26}$$

Furthermore, (3.24) is equivalent to:

$$\mathrm{Re}\left\{(1+\beta P(j\omega))\overline{(1+\alpha P(j\omega))}\right\} > 0, \quad \forall \omega \geq 0$$

thus in particular

$$\mathrm{Re}\left\{(1+\beta P(0))(1+\alpha P(0))\right\} > 0$$

i.e.

$$(1-\beta CA^{-1}B)(1-\alpha CA^{-1}B) > 0$$

or

$$\left(\frac{1}{CA^{-1}B} - \beta\right)\left(\frac{1}{CA^{-1}B} - \alpha\right) > 0$$

which contradicts (3.26), completing the proof. ◇

4

The servo problem for piecewise linear systems

4.1 Introduction

Behavior of trajectories for piecewise linear systems, in presence of an input signal, is an important issue from a control theoretic point of view. Most analysis results on piecewise linear systems are oriented toward stability of the origin for the unforced system [DeCarlo *et al.*, 2000],[Hassibi and Boyd, 1998],[Johansson and Rantzer, 1998]. The convergence of trajectories of the *unforced piecewise linear system* as defined in [Johansson and Rantzer, 1998] is not sufficient in general, to guarantee good behavior when input signals are applied to the system. Even if the unforced system is proved to be *stable*, applying an input might change the equilibrium point in such a way that the system behavior becomes unsatisfactory.

The servo problem for a general nonlinear system can be analyzed in a framework presented in Figure 4.1. The problem is to obtain information about the differences between the system's trajectories (x) and a predetermined trajectory x_r in presence of an input signal r. The exogenous input considered in this framework will be the time derivative of r. Choosing $\mathcal{L}_2$ norm as measure for the signals, it is natural to use the $\mathcal{L}_2$ gain to characterize the system behavior. Thus by computing

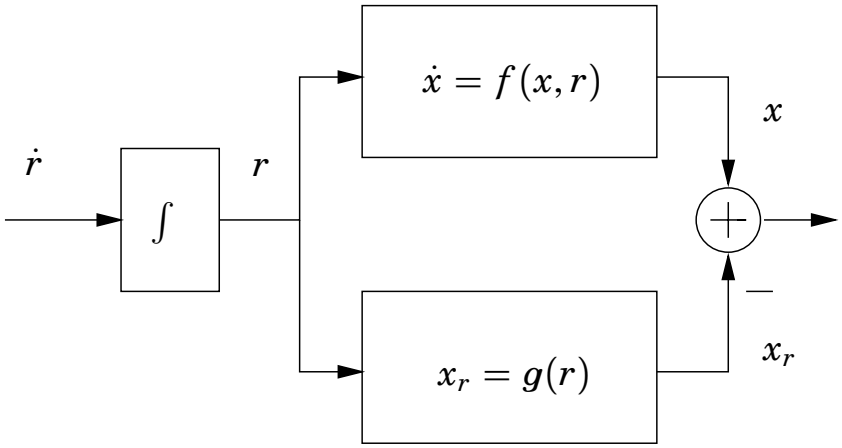

Figure 4.1 This chapter derives computable bounds on the map from the time derivative $\dot{r}$ of the reference signal to the magnitude $|x - x_r|$ of the state error.

the $\mathcal{L}_2$ gain from the derivative of the input signal $(\dot{r})$ to the "distance" between system trajectory (x) and reference trajectory (x_r), one obtains information relating the convergence of the system trajectories. In the literature on nonlinear systems, there exist qualitative results [Khalil, 1992], [Rugh and Shamma, 2000], of the following type: if an autonomous nonlinear system depending on some parameter, is stable for different fixed values of this parameter, then slow variations of the parameter between these fixed values, results in a non-autonomous system that will stay in the neighborhood of the equilibria defined by the fixed parameters. Our contribution is to give a quantitative bound on the neighborhood of the equilibria when the variation of the parameter is a continuous function. For piecewise linear systems a computational method using convex optimization is proposed.

This chapter contains the work in [Solyom and Rantzer, 2002b]. The layout of the chapter is as follows: the second section presents the related problem for a linear system while the third section generalizes the problem for a nonlinear system. Section 4.4 treats the case of piecewise linear systems. Finally, some conclusions are presented in Section 4.5.

4.2 The linear case

The $\mathcal{L}_2$ gain for a linear system is given by well known formulas. One approach is to solve a Riccati inequality, by means of convex optimization [Zhou and Doyle, 1998]. In Theorem 4.1, this approach is used for the computation of $\mathcal{L}_2$ gain between the reference signal's derivative and the difference $x - x_r$.

THEOREM 4.1
Consider the linear system:

$$\dot{x} = Ax + Br, \ x(0) = 0 \tag{4.1}$$

such that A^{-1} exists. Furthermore, define

$$x_r \stackrel{\Delta}{=} -A^{-1}Br \tag{4.2}$$

then the following statements are equivalent:

i) There exist $\gamma > 0, P > 0$ such that

$$\begin{bmatrix} A^T P + PA + I & PA^{-1}B \\ (A^{-1}B)^T P & -\gamma^2 I \end{bmatrix} < 0. \tag{4.3}$$

ii) For each solution of (4.1) with $r \in C^1$ and $r(0) = 0$ the following inequality holds:

$$\int_0^\infty |x - x_r|^2 \mathrm{dt} \leq \gamma^2 \int_0^\infty |\dot{r}|^2 \mathrm{dt} \tag{4.4}$$

□

Proof:
Define $\tilde{x} \stackrel{\Delta}{=} x - x_r$. Then $\dot{\tilde{x}} = A\tilde{x} + A^{-1}B\dot{r}$ For this system standard results can be applied to obtain (4.3).
Multiplying (4.3) by $\begin{bmatrix} x - x_r \\ \dot{r} \end{bmatrix}$ from the right and its transpose from the left gives

$$\frac{dV}{dt} + |x - x_r|^2 - \gamma^2 |\dot{r}|^2 < 0.$$

Integration gives (4.4). See [Zhou and Doyle, 1998] for details. ◇

4.3 The generic nonlinear case

In case of a general nonlinear system with a time varying input, it is more difficult to draw conclusions about trajectory convergence. Still, it is possible to find an upper bound on the $\mathcal{L}_2$ gain from the derivative of the input to the state deviation.

THEOREM 4.2
Let $f : \mathbb{R}^n \times \mathbb{R}^m \to \mathbb{R}^n$ be locally Lipschitz. For every $r \in \mathcal{R} \subset \mathbb{R}^m$ let $x_r \in \mathbb{R}^n$ be a unique solution to $0 = f(x_r, r)$.

If there exists $\gamma > 0$ and a non-negative C^1 function V, with $V(x_r, r) = 0$ for all $r \in \mathcal{R}$ and

$$\begin{bmatrix} \frac{\partial V}{\partial x} f(x,r) + |x - x_r|^2 & \frac{1}{2}\frac{\partial V}{\partial r} \\ \frac{1}{2}\left(\frac{\partial V}{\partial r}\right)^T & -\gamma^2 I \end{bmatrix} < 0 \tag{4.5}$$

for all $(x, r) \in \mathcal{S}$, then for each solution to

$$\dot{x} = f(x,r),\ x(0) = x_{r_0},\ r(0) = r_0 \tag{4.6}$$

such that $r(t) \in \mathcal{R}$ and $(x(t), r(t)) \in \mathcal{S}$ for all t, it holds that

$$\int_0^T |x - x_r|^2 \mathrm{dt} \leq \gamma^2 \int_0^T |\dot{r}|^2 \mathrm{dt} \tag{4.7}$$

□

Proof:
Multiplying (4.5) from left and right with $[\,\mathbf{1} \quad \dot{r}^T\,]$ one obtains:

$$\frac{\partial V}{\partial x} f(x,r) + |x - x_r|^2 + \frac{\partial V}{\partial r}\dot{r} - \gamma^2 |\dot{r}|^2 < 0$$

that is

$$\frac{dV}{dt} + |x - x_r|^2 - \gamma^2 |\dot{r}|^2 < 0$$

which in turns by integration on $[0,\, T]$ gives

$$V(x(T), r(T)) + \int_0^T |x - x_r|^2 \mathrm{dt} - \gamma^2 \int_0^T |\dot{r}|^2 \mathrm{dt} < 0$$

and inequality (4.7) results since $V(x,r) \geq 0$. $\diamond$

Remark Consider a linear system as in (4.1) with x_r defined by (4.2). Furthermore, consider a Lyapunov function of the form $V(x,r) = (x - x_r)^T P(x - x_r)$. Then

$$\frac{\partial V}{\partial x} f(x,r) \overset{(4.2)}{=} (x - x_r)^T (A^T P + PA)(x - x_r)$$
$$\frac{\partial V}{\partial r} = 2(x - x_r)^T P A^{-1} B$$

and the matrix in (4.5) becomes:

$$\begin{bmatrix} x - x_r & 0 \\ 0 & \mathbf{1} \end{bmatrix}^T \begin{bmatrix} A^T P + PA + I & PA^{-1}B \\ (A^{-1}B)^T P & -\gamma^2 I \end{bmatrix} \begin{bmatrix} x - x_r & 0 \\ 0 & \mathbf{1} \end{bmatrix}$$

which negative definiteness is given by (4.3).

Remark The matrix inequality (4.5) using Schur complement can be written as

$$\frac{\partial V}{\partial x} f(x,r) + \frac{1}{2\gamma^2} \frac{\partial V}{\partial r} \left(\frac{\partial V}{\partial r} \right)^T + \frac{1}{2}(x - x_r)^T (x - x_r) \leq 0$$

which is the Hamilton-Jacobi inequality for the system

$$\begin{cases} \begin{bmatrix} \dot{x} \\ \dot{r} \end{bmatrix} = \begin{bmatrix} f(x,r) \\ 0 \end{bmatrix} + \begin{bmatrix} 0 \\ 1 \end{bmatrix} u \\ y = x - x_r \end{cases} \tag{4.8}$$

(see Theorem 6.5 in [Khalil, 1992]).

Similarly to Theorem 4.2, an upper bound on the instantaneous value of $|x - x_r|$ can be obtained. The following result is analogous to Theorem 4.2.

THEOREM 4.3
Let $f : \mathbb{R}^n \times \mathbb{R}^m \to \mathbb{R}^n$ be locally Lipschitz. For all $r \in \mathcal{R} \subset \mathbb{R}^m$, let $x_r \in \mathbb{R}^n$ be a unique solution to $0 = f(x_r, r)$.

If there exist $\gamma, c, p > 0$ and a C^1 function V with $V(x,r) \geq c|x - x_r|^p$ and

$$\begin{bmatrix} \frac{\partial V}{\partial x} f(x,r) + \lambda V & \frac{1}{2}\frac{\partial V}{\partial r} \\ \frac{1}{2}\left(\frac{\partial V}{\partial r}\right)^T & -\gamma^2 I \end{bmatrix} < 0 \tag{4.9}$$

for all $(x,r) \in \mathcal{S}$, then for each solution to

$$\dot{x} = f(x,r),\ x(0) = x_{r_0},\ r(0) = r_0 \tag{4.10}$$

such that $r(t) \in \mathcal{R}$ and $(x(t), r(t)) \in \mathcal{S}$, it holds that

$$|x(T) - x_r(T)|^p \leq \frac{\gamma^2}{c} \int_0^T |\dot{r}|^2 e^{-\lambda(T-t)} \mathrm{d}t \tag{4.11}$$

□

Proof:
Multiplying (4.5) from left and right with $[\,\mathbf{1} \quad \dot{r}^T\,]$ one obtains:

$$\frac{\partial V}{\partial x} f(x,r) + \frac{\partial V}{\partial r}\dot{r} + \lambda V - \gamma^2 |\dot{r}|^2 < 0$$

thus on $\mathcal{S}$ yields:

$$\frac{dV}{dt} + \lambda V - \gamma^2 |\dot{r}|^2 < 0$$

which by multiplication with $e^{-\lambda(T-t)} > 0$ gives

$$\begin{aligned} &\frac{dV}{dt} e^{-\lambda(T-t)} + \lambda V e^{-\lambda(T-t)} - \gamma^2 |\dot{r}|^2 e^{-\lambda(T-t)} < 0 \\ \Leftrightarrow &\frac{d}{dt} V e^{-\lambda(T-t)} - \gamma^2 |\dot{r}|^2 e^{-\lambda(T-t)} < 0 \end{aligned}$$

then by integrating on $[0,\ T]$ and using that $V(x(0), r(0)) = 0$, gives

$$\begin{aligned} c^2 |x(T) - x_r(T)|^p &\leq V(x(T), r(T)) < \\ &< \gamma^2 \int_0^T |\dot{r}|^2 e^{-\lambda(T-t)} \mathrm{d}t \end{aligned}$$

thus inequality (4.11) yields. ◇

Remark Consider a linear system as in (4.1) with x_r defined by (4.2) and $\mathcal{S} = \mathbb{R}^n \times \mathbb{R}^m$. Furthermore, consider a Lyapunov function of the form $V(x,r) = (x - x_r)^T P(x - x_r)$ and $p = 2$. Then the Lyapunov function's positivity condition in Theorem 4.3 translates to:

$$P - c^2 I > 0 \Leftrightarrow \begin{bmatrix} P & I \\ I & \frac{1}{c^2} I \end{bmatrix} > 0$$

while (4.9) becomes:

$$\begin{bmatrix} A^T P + PA + \lambda P & PA^{-1}B \\ (A^{-1}B)^T P & -\gamma^2 I \end{bmatrix} < 0$$

Obviously, for a generic nonlinear system as considered in (4.6) it might be difficult to find a $V(x,r)$ such that (4.5) or (4.9) is fulfilled. In case of piecewise linear systems convex optimization can be used in the analysis.

4.4 Piecewise linear system

Consider now a particular kind of nonlinear systems, a piecewise linear system, of the form:

$$\dot{x} = A_i x + B_i r, \quad x(t) \in X_i \tag{4.12}$$

with $\{X_i\}_{i \in I} \subseteq \mathbb{R}^n$ a partition of the state space into a number of convex polyhedral cells with disjoint interior. Suppose that for any constant $r \in \mathcal{R}$, the piecewise linear system has a unique equilibrium point.

Furthermore, consider symmetric matrices S_{ij} that satisfy the inequality:

$$\begin{bmatrix} x - x_r \\ r \end{bmatrix}^T S_{ij} \begin{bmatrix} x - x_r \\ r \end{bmatrix} > 0, \; x \in X_i, \; r(t) \in \mathcal{R}_j \text{ for all } t \tag{4.13}$$

Define

$$\bar{B}_j \triangleq \begin{bmatrix} A_j^{-1} B_j \\ 1 \end{bmatrix}, \qquad \bar{I} \triangleq \begin{bmatrix} I_n & 0 \\ 0 & 0_m \end{bmatrix} \tag{4.14}$$

$$\bar{A}_{ij} \triangleq \begin{bmatrix} A_i & -A_i A_j^{-1} B_j + B_i \\ 0 & 0 \end{bmatrix} \tag{4.15}$$

The following proposition is useful for application of Theorem 4.2 and Theorem 4.3.

PROPOSITION 4.1
Let $f(x,r) = A_i x + B_i r$, $x_r = -A_j^{-1} B_j r$ with $x(0) = x_r(0)$, $r(0) = r_0$. If there exist $\gamma > 0$, $P > 0$ such that $\bar{P} = \text{diag}\{P, 0\}$ satisfies

$$\begin{bmatrix} \bar{A}_{ij}^T \bar{P} + \bar{P}\bar{A}_{ij} + S_{ij} + \bar{I} & \bar{P}\bar{B}_j \\ \bar{B}_j^T \bar{P} & -\gamma^2 I \end{bmatrix} < 0,\ i \neq j \tag{4.16}$$

$$\begin{bmatrix} A_j^T P + P A_j + I & P A_j^{-1} B_j \\ (A_j^{-1} B_j)^T P & -\gamma^2 I \end{bmatrix} < 0 \tag{4.17}$$

then $V(x,r) = (x - x_r)^T P (x - x_r)$ satisfies (4.5) for all $x \in X_i$, $r(t) \in \mathcal{R}_j$. □

In particular, in the case when $\dot{r}(t) = 0$, for $t > T$, by finding a finite $\gamma > 0$ it is shown that all trajectories of the nonlinear system (4.12) will converge to x_r.

Remark When the local linear systems contain affine terms the argument vector of the Lyapunov function will be extended to $[\tilde{x} \quad r \quad 1]$. Similarly, when partitions that do not contain the origin are to be described, the argument vector will be augmented.

The conservatism of the theorems can be reduced by considering piecewise quadratic Lyapunov function. In this case the Lyapunov function will be piecewise C^1 instead of C^1. Imposing that is non-increasing at the points of discontinuity, the results yield (see [Johansson and Rantzer, 1998]).

Remark The variation in the affine term due to r, can be viewed as parametric uncertainty in the system. Thus the theorem can be used to prove robust stability for a piecewise linear system, with uncertain affine terms in the local linear systems.

EXAMPLE 4.1
Consider the system of the form:

$$\dot{x} = Ax + B(r - \varphi(Cx))$$

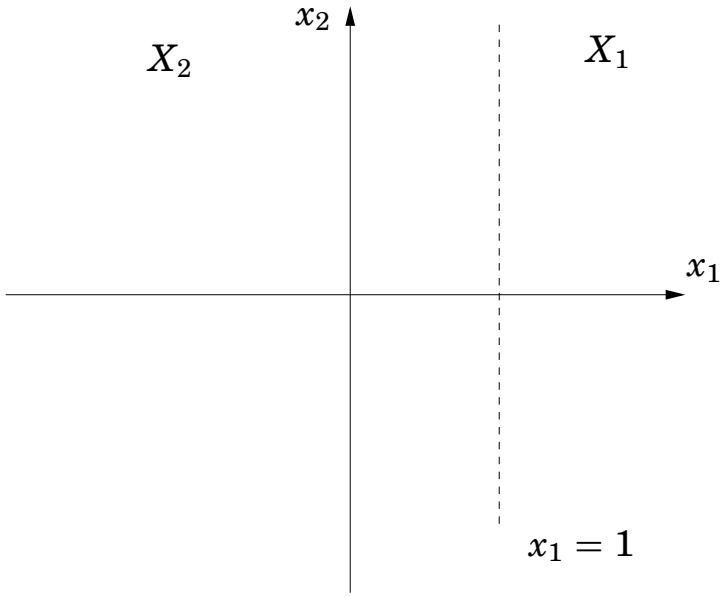

Figure 4.2 State space partitions of the system in Example 4.1.

where A is a stable matrix. The nonlinearity is defined as:

$$\varphi(x) = \begin{cases} x, & x < 1 \\ 1, & x \geq 1 \end{cases}$$

This system can be described by the following piecewise linear system.

$$\dot{x} = \begin{cases} Ax - B + Br, \; Cx \geq 1 \\ (A - BC)x + Br, \; Cx < 1 \end{cases} \tag{4.18}$$

The state space partitions of such a system (where the subsystems are of second order and $C = [1 \quad 0]$) is shown in Figure 4.2. Here $X_1 = \{x | Cx \geq 1\}$ and $X_2 = \{x | Cx < 1\}$. The numerical values are:

$$A = \begin{bmatrix} -0.5 & 1 \\ -1 & 0 \end{bmatrix}, \; B = \begin{bmatrix} 1 \\ 3 \end{bmatrix}$$

Then the sets $\mathcal{R}_1 = (\frac{4}{3}, \infty)$ and $\mathcal{R}_2 = (-\infty, \frac{4}{3})$ follow from simple computations.

Consider first the case when $r(t) \in \mathcal{R}_2$ for all t, i.e. $x_r(t) \in X_2$ for all t .
The LMIs resulting from Theorem 4.2 turn out to be infeasible, suggesting that a quadratic Lyapunov function might be too conservative. Therefore a piecewise quadratic Lyapunov function is tried (see [Johansson and Rantzer, 1998]) :

$$V(x,r) = \begin{cases} \begin{bmatrix} x - x_r \\ r \\ 1 \end{bmatrix}^T P_1 \begin{bmatrix} x - x_r \\ r \\ 1 \end{bmatrix}, \ x \in X_1 \\ (x - x_r)^T P_2 (x - x_r), \ x \in X_2 \end{cases}$$

Minimizing γ subject to the LMI constraints, one obtains the Lyapunov function's matrices:

$$P_1 = \begin{bmatrix} 5.0749 & -0.8930 & -6.6918 & 8.9351 \\ -0.8930 & 5.1082 & 0.0703 & 0.2583 \\ -6.6918 & 0.0703 & -12.1141 & 16.2238 \\ 8.9351 & 0.2583 & 16.2238 & -2.2493 \end{bmatrix}$$

$$P_2 = \begin{bmatrix} 20.69 & -0.63 \\ -0.63 & 5.1 \end{bmatrix}$$

and $\gamma = 7.182$.

Consider now the case when $r(t) \in \mathcal{R}_1$ for all t, i.e. $x_r(t) \in X_1$ for all t.

Consider the Lyapunov function:

$$V(x,r) = \begin{cases} (x - x_r)^T P_1 (x - x_r), \ x \in X_1 \\ \begin{bmatrix} x - x_r \\ r \\ 1 \end{bmatrix}^T P_2 \begin{bmatrix} x - x_r \\ r \\ 1 \end{bmatrix}, \ x \in X_2 \end{cases}$$

Solving the constrained minimization problem, one obtains the Lyapunov function's matrices:

$$P_2 = \begin{bmatrix} 18.36 & -2.55 & 47.17 & -68.64 \\ -2.55 & 4.22 & -13.32 & 8.21 \\ 47.17 & -13.32 & 146.8 & -173.34 \\ -68.64 & 8.21 & -173.34 & 317.36 \end{bmatrix}$$

$$P_1 = \begin{bmatrix} 3.874 & -0.503 \\ -0.503 & 4.225 \end{bmatrix}$$

and $\gamma = 8.3221$.

Thus for every (x, r) starting in $X_1 \times \mathcal{R}_1$ respectively in $X_2 \times \mathcal{R}_2$, trajectory convergence, in the sense of Theorem 4.2, is guaranteed by the finite γ's.

It is of interest to derive lower bounds on the $\mathcal{L}_2$ gain in order to verify the conservativeness of the result. A natural lower bound is obtain by Theorem 4.1. This way for the case when $x_r \in X_2$ a lower bound of 1.12 is obtained, while in the case $x_r \in X_1$ a lower bound of 8.318 is computed. For the case when $x_r \in X_1$ the resulting bounds turned out to be very tight. However, it can be noticed that the lower bound when $x_r \in X_2$ is rather small in comparison to the upper bound. This could be refined by finding a "worst case disturbance" for the nonlinear system.

In Figure 4.3 state trajectories x_1 and x_2 are presented when $r \in \mathcal{R}_2$. Notice that x_1 is passing through region X_1.

As seen above, *S-procedure* is used (S_i) to describe the state-space partition of (4.12), and in the same time describe the set of considered r's. More details on how to find such matrices can be found in [Johansson and Rantzer, 1998]. The used matrices are: for X_1

$$S_{12} = \begin{bmatrix} 0 & 0 & -8.562 & 11.772 \\ 0 & 0 & 0 & 0 \\ -8.562 & 0 & -12.844 & 16.259 \\ 11.772 & 0 & 16.259 & -20.528 \end{bmatrix}$$

and for X_2

$$S_{21} = \begin{bmatrix} 0 & 0 & -52.66 & -34.957 \\ 0 & 0 & 0 & 0 \\ -52.66 & 0 & -315.965 & 100.217 \\ -34.957 & 0 & 100.217 & -336.966 \end{bmatrix}$$

□

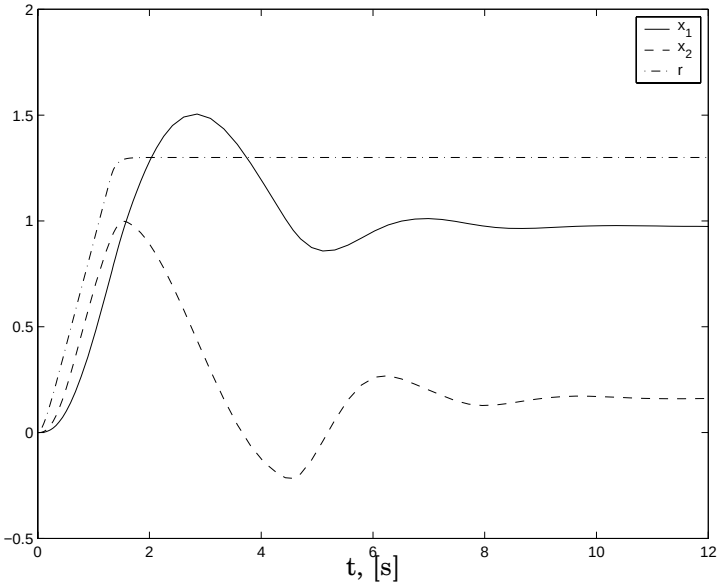

(a) System trajectories and input signal.

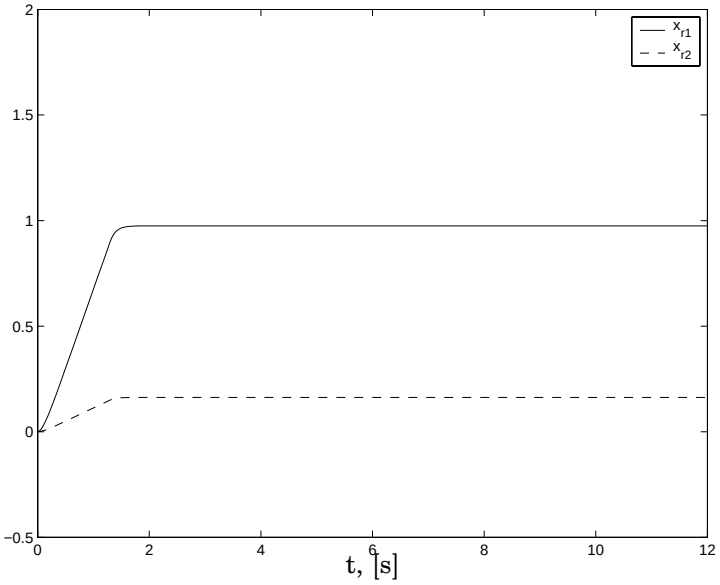

(b) Reference trajectories.

Figure 4.3 Simulation results for the system in Example 4.1.

4.5 Conclusions

Trajectory convergence in presence of constant and time varying inputs has been studied. Quantitative result has been established for a sufficient condition regarding trajectory convergence for a class of nonlinear systems, where one of the parameters (r) is time varying. This result has been used for piecewise linear systems, where Proposition 4.1 in combination with Theorem 4.2, give a tool for computing an upper bound on the $\mathcal{L}_2$ gain from $\dot{r}$ to $x - x_r$, characterizing the servo problem for such systems.

5

Bibliography

Åström, K. J. (1997): "Limitations on control system performance." In *European Control Conference*. Brussels, Belgium.

Åström, K. J. and T. Hägglund (1995): *PID Controllers: Theory, Design, and Tuning*, second edition. Instrument Society of America, Research Triangle Park, North Carolina.

Åström, K. J., H. Panagopoulos, and T. Hägglund (1998): "Design of PI controllers based on non-convex optimization." *Automatica*, **34:5**, pp. 585–601.

Bakker, E., H. B. Pacejka, and L. Lidner (1989): "A new tire model with application in vehicle dynamics studies." *SAE, 890087*.

Bliman, P. A., T. Bonald, and M. Sorine (1995): "Hysteresis Operators and Tire Friction Models: Application to vehicle simulation." In *Proceedings of ICIAM'95, Hamburg, Germany*.

Buckman, L. C. (1998): *Commercial Vehicle Braking Systems: Air Brakes, ABS and Beyond*. The 43rd L. Ray Buckendale Lecture. Society of Automotive Engineers, Inc.

Canudas de Wit, C. and P. Tsiotras (1999): "Dynamic Tire Friction Models." In *Proceedings of the IEEE Conference on Decision and Control, Phoenix*, pp. 3746–3751.

DeCarlo, R. A., M. S. Branicky, S. Pettersson, and B. Lennartson (2000): "Perspectives and Results on the Stability and Stabilizability of Hybrid Systems." *Proceedings of IEEE*, pp. 1069 – 1082.

Drakunov, S., Ü. Özgüner, P. Dix, and B. Ashrafi (1995): "ABS control using optimum search via sliding mode." In *IEEE Transactions on Control System Technology*, vol. 3, pp. 79–85.

Hassibi, A. and S. Boyd (1998): "Quadratic Stabilization and Control of Piecewise-Linear Systems." *Proceedings of the American Control Conference*, pp. 3659 – 3664.

Hattwig, P. (1993): "Synthesis of ABS hydraulic systems." *SAE, 930509*.

Jiang, F. (2000): *A novel control approach to a class of antilock brake problems*. PhD thesis, Cleveland State University.

Johansen, T., J. Kalkkuhl, J. Lüdemann, and I. Petersen (2001): "Hybrid Control Strategies in ABS." *Proceedings of the American Control Conference, Arlington*.

Johansson, M. and A. Rantzer (1998): "Computation of piecewise quadratic Lyapunov functions for hybrid systems." *IEEE Transactions on Automatic Control*, **43:4**, pp. 555–559. Special issue on Hybrid Systems.

Kalkkuhl, J. (2001): "Demonstrator Application Benchmark, Heterogeneous Hybrid Control: $\mathcal{H}^2C$." Technical Report. DaimlerChrysler AG.

Kalkkuhl, J., T. A. Johansen, J. Lüdemann, and A. Queda (2000): "Nonlinear adaptive backstepping with estimator resetting using multiple observers." *Submitted for publication*.

Khalil, H. K. (1992): *Nonlinear Systems*. MacMillan, New York.

Kiencke, U. and L. Nielsen (2000): *Automotive Control Systems*. Springer Verlag.

Liu, Y. and J. Sun (1998): "Target slip tracking using gain-scheduling for braking systems." In *Proceedings of the American Control Conference, Seatle, Washington*, pp. 1178–1182.

Maier, M. and K. Müller (1995): "ABS5.3: The new and compact ABS5 unit for passenger cars." *SAE, 930757*.

Maisch, W., W.-D. Jonner, R. Mergenthaler, and A. Sigi (1993): "ABS5 and ASR5: The new ABS/ASR family to optimize directional stability and traction." *SAE, 930505*.

Panagopoulos, H. (2000): *PID Control, Design, Extension, Application*. PhD thesis, Lund Institute of Technology, Department of Automatic Control.

Panagopoulos, H., K. J. Åström, and T. Hägglund (1999): "Design of PID controllers based on constrained optimization." In *Proc. 1999 American Control Conference (ACC'99)*. San Diego, California. Invited paper.

Rugh, W. J. and J. S. Shamma (2000): "Research on gain scheduling." *Automatica*, pp. 1401 – 1425.

Saeki, M. and J. Kimura (1997): "Design method of robust PID controller and CAD systems." In *11th IFAC Simposium on System Identification*, pp. 1587–1593.

Slotine, J. J. and W. Li (1991): *Applied Nonlinear Control*. Prentice Hall, Englewood Cliffs, New Jersey.

Solyom, S. and A. Ingimundarson (2002): "A synthesis method of robust PID controllers for a class of uncertainties." *Accepted for publication in Asian Journal of Control, Special Issue on PID Control*.

Solyom, S. and A. Rantzer (2002a): "ABS Control by Gain Scheduling." *To be published in Nonlinear and Hybrid Control in Automotive Applications, Springer-Verlag*.

Solyom, S. and A. Rantzer (2002b): "The servo problem for piecewise linear systems." In *Accepted at 15th International Symposium on Mathematical Theory of Networks and Systems, Notre Dame*.

Åström, K. J. and T. Hägglund (1995): *PID Controllers: Theory, Design and Tuning*. The International Society of Measurement and Control.

Wellstead, P. and N. Pettit (1997): "Analysis and redesign of an antilock brake system controller." In *IEE Proceedings - Control Theory Appl.*, vol. 144, pp. 413–425.

Zhou, K. and J. C. Doyle (1998): *Essentials of robust control*. Prentice Hall.